THE ASTRONOMICAL JOURNAL, 122:1718–1735, 2001 October

MULTICOLOR PHOTOMETRY OF THE GALAXIES IN THE CENTRAL REGION OF ABELL 2634

QIRONG YUAN,[1,2,3] XU ZHOU,[1] JIANSHENG CHEN,[1] ZHAOJI JIANG,[1] JUN MA,[1] HONG WU,[1] SUIJIAN XUE,[1] AND JIN ZHU[1]

Received 2001 April 9; accepted 2001 July 11

ABSTRACT

An optical photometric observation with the Beijing-Arizona-Taipei-Connecticut multicolor system is carried out for the central region of the nearby cluster of galaxies Abell 2634. From the 2K × 2K CCD images with 14 filters, which cover a range of wavelength from 3600 to 10000 Å, 5572 sources are detected down to $V \sim 20$ mag in a field of $56' \times 56'$ centered on this regular cluster of galaxies. As a result, we achieved the spectral energy distributions (SEDs) of all sources detected. There are 178 previously known galaxies included in our observations, 147 of which have known radial velocities in the literature. After excluding the foreground and background galaxies, a sample of 124 known members is formed for an investigation of the SED properties. The comparison of observed SEDs of the early-type member galaxies with the template SEDs demonstrates the accuracy and reliability of our photometric measurements. Based on the knowledge of SED properties of member galaxies, we performed the selection of faint galaxies belonging to Abell 2634. It is well shown that the color-color diagrams are powerful in the star-galaxy separation. As a result, 359 faint galaxies are selected by their color features. The technique of photometric redshift and color-magnitude correlation for the early-type galaxies are applied for these faint galaxies, and a list of 74 faint member galaxies is achieved. On the basis of the newly generated sample of member galaxies, the spatial distribution and color-magnitude relation of the galaxies in the core region of Abell 2634 are discussed. There exists a tendency that the color index dispersion of the early-type members is larger for the outer region, which might reflect some clues about the environmental effect on the evolution of galaxies in a cluster.

Key words: galaxies: clusters: individual (Abell 2634) — galaxies: distances and redshifts — galaxies: fundamental parameters

1. INTRODUCTION

It is widely appreciated that the observations of galaxy clusters can provide useful constraints on the theories of formation and evolution of large-scale structure, since they are the largest gravitationally bound systems in the universe. A great volume of observational data has been achieved for the galaxies belonging to a cluster, particularly for the nearby clusters of galaxies. The rich cluster of galaxies, Abell 2634, is one example. Extensive observational efforts are being made to expand the kinematic database for Abell 2634 because it has many intriguing observational features. First, its central galaxy, NGC 7720, classified as a cD galaxy first by Matthews, Morgan, & Schmidt (1964) and then as a D galaxy by Dressler (1980a), was found to have a companion galaxy, namely NGC 7720A, with a projected distance of 7.2 h_{75}^{-1} kpc and a velocity difference of about 1000 km s^{-1}. Second, a surprisingly large negative peculiar velocity for Abell 2634 was derived when the fundamental plane (FP) relation D_n-σ (Dressler et al. 1987) was sketchily extended to estimate the distance of Abell 2634 (Lucey et al. 1991), which is challengable for the universality of the FP and Tully-Fisher (TF) relations. With the effort for several years of Lucey et al. (1997) and Scodeggio, Giovanelli, & Haynes (1997), larger samples of member galaxies with more accurate photometric measurements (including I-band observations) are constructed. Abell 2634 was found to have a negligibly small peculiar velocity with respect to the cosmic microwave background reference frame. The FP distance estimate of Abell 2634 is in good agreement with that given by the TF relation.

Additionally, the prototypical wide-angle tailed radio source, 3C 465, is found to coincide with the central cD galaxy, NGC 7720 (Griffen 1963; Eilek et al. 1984; O'Donoghue, Owen, & Eilek 1990). A study of this cluster by Pinkney et al. (1993) suggested that the large-scale turbulent gas motions fueled by a cluster-subcluster merging process might be responsible for the observed bending of radio tails. To investigate issues related to the kinematics of NGC 7720, Scodeggio et al. (1995; hereafter SSGH) carried out the multifiber spectroscopy and 21 cm line observations and particularly analyzed the structure, kinematics, and morphological segregation of galaxies within the central half-degree region (HDR). There are 99 member galaxies brighter than $m_v \sim 16.0$ in the inner 0°.5 region, which is called the HDR sample. The completeness of the inner region of 1 deg^2 reached $m_{pg} \sim 16.0$. As a result, the morphological dependence of spatial and kinematic properties was found: the early-type galaxies appear to be a relaxed system, while the spiral galaxies have a much larger velocity dispersion.

Studies of the luminosity function of cluster galaxies show that most intrinsically bright galaxies in clusters, $M_B < -16$, are giant elliptical galaxies. Down to $m_v \sim 18.5$ in Abell 2634, the majority of apparently faint member galaxies are still intrinsically bright. There should be many giant elliptical galaxies within the apparent magnitude range of $16.0 < m_v < 18.5$. In order to enrich our understanding of the structure and dynamics of Abell 2634, these faint member galaxies should be taken into account.

[1] National Astronomical Observatories, Chinese Academy of Sciences, Beijing 100012, China; zhouxu@vega.bac.pku.edu.cn, chen@vega.bac.pku.edu.cn.

[2] Department of Physics, Nanjing Normal University, NingHai Road 122, Nanjing 210097, China; qirongwy@public1.ptt.js.cn.

[3] Visiting Astronomer, National Optical Astronomy Observatories, Tucson, AZ 85726; under contract to China Scholarship Council; yuan@noao.edu.

However, the spectroscopic observations are not available yet for a great number of galaxies fainter than 16.0 mag in Abell 2634. The multicolor optical photometric observation therefore becomes a common alternative means for studying some properties of the member galaxies, such as the color-magnitude relation (Bower, Lucey, & Ellis 1992), the Butcher-Oemler effect (Butcher & Oemler 1978), and the morphology-density relation (Dressler 1980b).

Due to a large field of view, the Schmidt Telescope (1 m class), equipped with a large-format CCD, is one of most suitable facilities for obtaining photometric data for the nearby clusters of galaxies. The multicolor photometry can provide the spectral energy distributions (SEDs) of all the objects within the field of view. Comparing the integration times required for spectroscopy with a certain depth on a large telescope, the amount of observing times for multicolor photometry are much shorter and therefore more readily scheduled. The Beijing-Arizona-Taipei-Connecticut (BATC) multicolor photometric survey is designed to obtain the SED information of cluster galaxies and other types of objects (Fan et al. 1996). This paper will present the multicolor optical photometry of the central region of Abell 2634 using the 60/90 cm Schmidt Telescope of the Beijing Astronomical Observatory (BAO), with 14 BATC filters covering a wide wavelength range from 3800 to nearly 10000 Å. The comparison of observed SEDs for the previously known member galaxies with the template SEDs demonstrates the accuracy and reliability of our photometric measurements. Our multicolor photometry contains a large quantity of bright member galaxies with sufficiently small photometric errors, which allows a verification of color-magnitude correlation, as well as a testing application of the technique of photometric redshift. After performing a reliable star-galaxy separation by the color-color diagrams, we carried out a membership selection based on the SED features of known member galaxies. The technique of photometric redshift and color-magnitude correlation have provided useful constraints on the membership selection. As a result, we cataloged the SEDs of the newly selected faint members, based on which some properties of the enlarged sample of member galaxies can be addressed. We believe that current study will not only supplement the databases of member galaxies in this well-studied cluster, but also extend the investigations on the spatial distribution and color-magnitude relation of the galaxies in the core of Abell 2634 to an unprecedented depth.

This paper is structured as follows: In § 2, we will present our observations and data reduction, as well as the photometric catalogs of the objects (including the known member galaxies) in the central field of Abell 2634. The analysis of the SEDs for the known member galaxies is shown in § 3. An SED selection of faint member galaxies is given in § 4, and the spatial distribution and color properties of the enlarged sample of member galaxies is presented in § 5. Finally, we will give a summary in § 6. The cosmological parameters $H_0 = 50$ km s^{-1} Mpc^{-1} and $q_0 = 0.5$ have been assumed.

2. OBSERVATIONS AND DATA REDUCTION

2.1. *BATC Observations*

Abell 2634 is a nearby ($z \sim 0.03$) regular cluster of galaxies, classified by Abell (1958) as of richness class 1. Dressler (1980a) listed 132 galaxies in his catalog, and the fraction of early-type galaxies (E/S0) is about 63%. In the HDR sample of SSGH, the fraction of early-type galaxies reaches ~71%. This cluster appears to be at a distance of ~9000 km s^{-1}, projected on the main ridge of the Pisces-Perseus Supercluster (PPS; see Fig. 1 in Wegner, Haynes, & Giovanelli 1993). Its companion, Abell 2666, is closely located at approximately 3° to the east, with a heliocentric redshift of ~8154 km s^{-1} (Struble & Rood 1999).

Our multicolor optical photometry concentrates on a region of 56 × 56 arcmin^2 centered on NGC 7720. The 60/90 cm f/3 Schmidt Telescope of BAO, located at the Xinglong site with an altitude of 900 m, was used to obtain the photometric observations. A Ford 2048 × 2048 CCD camera was equipped at the prime focus of the telescope. The field of view was 0.95 deg^2, and the spatial scale was 1.″67 pixel^{-1}. The details of the Schmidt Telescope, CCD camera, and data acquisition system can be found elsewhere (Fan et al. 1996; Yan et al. 2000). We make use of the BATC filter system, which includes 16 intermediate-band filters covering the whole optical wavelength range from ~3000 to 10000 Å. The transmissions of these filters can been seen in Figure 1 of Zhou et al. (2001).

Only 14 filters, from *b* to *p*, were used for the observations of Abell 2634. The filter number, filter name, effective wavelength centroid, and FWHM for each filter are listed in Table 1. In total, we have made more than 40 hr of exposures and obtained 214 images on the central region of Abell 2634. After a check of the image quality, 173 images with nearly 36 hr of exposure were selected to be combined. The combined images cover an area defined by a right ascension range from $23^h36^m16^s$ to $23^h40^m23^s$ and a declination range from 26°33′30″ to 27°30′01″ (for the J2000 equinox). The seeing of the combined images were quite different from band to band, but the typical seeing of the combined image for each filter band was about 5″.

Almost all nights were thought to be photometric by the observers. The standard stars were observed between air masses of 1 and 2 for each program filter band. Normally, four to six filters were selected to make flux calibrations during each photometric night. The standard stars were put near the CCD center and only 300 × 300 subimages were taken for the standard stars to save readout time and disk space. The extinction coefficient and magnitude zero point obtained from standard stars were used for making the flux calibration on the BATC field images. The details of the observation for calibration are described in Yan et al. (2000). Table 1 also gives the parameters for our observations.

2.2. *Data Reduction*

The bias subtractions and dome flat-field corrections were done on the CCD images. The cosmic-ray and bad-pixel effects were corrected by comparing the images. The images were recentered, and position calibration was performed by using the Guide Star Catalog. The fluxes of the intermediate-band filter images were calibrated by Oke & Gunn standard stars (Oke & Gunn 1983; Fukugita et al. 1996).

As in other works on this image field, we are preparing the SED catalog of sources. The magnitudes were measured by the aperture photometry with a detection threshold of 4 σ of the sky fluctuation per pixel. A minimum of 1 pixel above the threshold was required for detection. This might introduce a false detection, particularly for the nearby very

TABLE 1

PARAMETERS OF THE BATC FILTERS AND THE STATISTICS OF OUR OBSERVATIONS

No.	Filter Name	Central λ (Å)	FWHM (Å)	Exposure (s)	Number of Images	Seeing[a] (arcsec)	Calibration Images	Stars Detected	Limiting Magnitude
1	*b*	3890	291	23100	29	5.36	3	1427	19.5
2	*c*	4210	309	3600	3	6.12	0[b]	2190	20.0
3	*d*	4550	332	4500	6	5.29	3	3050	20.5
4	*e*	4920	374	13980	15	3.94	3	3561	20.5
5	*f*	5270	344	6540	16	4.70	3	3010	20.0
6	*g*	5795	289	8400	7	5.90	4	3837	20.0
7	*h*	6075	308	5340	14	4.09	6	3919	19.5
8	*i*	6660	491	6320	12	5.02	6	3910	19.5
9	*j*	7050	238	4210	16	4.21	4	4182	19.0
10...	*k*	7490	192	8880	10	3.77	4	5572	20.0
11...	*m*	8020	255	10960	13	4.46	3	4356	19.0
12...	*n*	8480	167	18480	16	4.80	1	3948	19.0
13...	*o*	9190	247	4740	6	3.78	0[b]	3432	18.5
14...	*p*	9745	275	8340	10	4.79	3	2220	17.5

[a] This column lists the seeings of the combined images.

[b] No calibration image was taken. The intrinsic magnitudes for the *c* and *o* filters are determined by the method of the SED model (Zhou et al. 1999).

bright stars. Since most of galaxies in the images are obviously extended, we finally selected a fixed aperture of 5 pixels to do the photometry, which is large enough to make different seeing effects negligible. Although the resulting magnitudes given by photometry with fixed aperture are not the same as the total magnitudes of galaxies in the literature, this is a proper way to obtain the reliable color indices (i.e., relative SEDs) of all the sources. The photometry program developed by Bertin & Arnouts (1996), SExtractor (Version 2.1.6) namely, was used for the photometry. During extraction of the sources, a filter of 3×3 "all-ground" convolution mask with a FWHM = 2 pixels was used. Since the adopted aperture size is rather large, contamination of the light by nearby objects may sometimes not be negligible. The number of sources detected in the combined images are shown in Table 1.

We used four standard stars, namely BD $+17°4708$, BD $+26°2606$, HD 19445, and HD 84937, in Oke & Gunn (1983) for the BATC flux calibration. The absolute fluxes of these stars were taken from Fukugita et al. (1996). The definitions of BATC magnitudes are in the AB_ν system of Oke & Gunn (1983): $m_{\rm BATC} = -2.5 \log \tilde{F}_\nu - 48.6$. Once the aperture photometry on the images of standard stars is done, the extinction coefficients, K, and magnitude zero points, C, can be obtained by fitting the extinction curve of magnitude versus air mass: $m_{\rm inst} - m_{\rm BATC} = KX + C$, where X is the air mass of the image. The values of K and C were derived by a median fitting of the data points with a straight line. The procedures of flux calibration are detailed in Zhou et al. (2001).

For *c* and *o* filters, we do not have the calibration images. Fortunately, we developed a method to calibrate the SEDs of objects for our large field multicolor photometric system based on the SED library (Zhou et al. 1999), which is the so-called model calibration. This method heavily improved the quality of the observations taken under not-so-perfect photometric conditions. The SED calibration was done for our combined images. Then we derived the calibrated magnitudes in the *c* and *o* bands from the information of the calibrated SEDs. For other filter bands, the magnitudes derived by ordinary standard calibrations were adopted for further analyses.

2.3. *Photometric Catalog*

We achieved the photometric magnitudes within 14 filter bands for 5572 sources in the central region ($56' \times 56'$) of Abell 2634. This SED catalog will be electronically provided upon request. To cross identify all the known galaxies within our field, we made use of the NASA/IPAC Extragalactic Database (NED). As a result, 178 known galaxies were found to have counterparts in our SED catalog. The identification is unambiguous for a majority of these galaxies, according to their positional offsets and apparent magnitudes. The SEDs of these 178 galaxies are cataloged in Table 2, which is structured as follows:

Column (1): Number of the galaxies, sorted by the R.A. in the J2000 epoch.

Columns (2) and (3): R.A. and decl. in the J2000 epoch given by our photometric measurements.

Column (4): Redshift, in kilometers per second, provided by NED.

Column (5): Membership code. Member galaxies are identified as "m," foreground galaxies are marked as "f," background galaxies are marked by "b," and a "?" means possible membership (see text for details).

Columns (6)–(19): Photometric magnitudes in *b*- through *p*-filter bands. The value of 0.0 means no detection in this filter band.

It should be noted that the photometric magnitudes given in Table 2 might be somewhat different from the total magnitudes of galaxies given in some catalogs, since we used a fixed aperture to do the photometry. What we attempted to obtain was the relative SEDs of objects in the central region of Abell 2634.

We checked two kinds of errors respectively given by the photometric program SExtractor and by a comparison with the stellar spectral templates of Gunn & Stryker (1983). The statistic errors given by the SExtractor are smaller than the real measurement errors. We compared the errors using different images with the same filter. By separating stars into different subgroups of magnitudes with an interval of 0.5 mag, the mean measurement errors at specified magnitudes were derived. We found that the measurement errors

TABLE 2

SED Catalog of 178 Known Galaxies in the Central Region of Abell 2634

No. (1)	R.A. (J2000) (2)	Decl. (J2000) (3)	*cz* (4)	*M* (5)	*b* (6)	*c* (7)	*d* (8)	*e* (9)	*f* (10)	*g* (11)	*h* (12)	*i* (13)	*j* (14)	*k* (15)	*m* (16)	*n* (17)	*o* (18)	*p* (19)
1	23 36 23.74	27 13 21.77	19666	b	19.11	18.69	18.36	17.95	17.83	17.30	17.21	17.04	16.90	16.74	16.60	16.61	16.40	16.37
2	23 36 26.11	27 23 55.79	9133	m	17.76	17.08	16.65	16.18	16.10	15.64	15.38	15.25	15.19	14.92	14.91	14.67	14.53	14.53
3	23 36 26.87	26 39 21.59	9212	m	18.47	18.03	17.95	17.71	17.54	17.30	17.26	17.07	17.01	16.90	16.86	16.85	16.81	16.52
4	23 36 27.61	27 02 17.90	...	?	19.36	18.94	18.45	18.05	17.77	17.48	17.27	17.08	16.94	16.80	16.67	16.62	16.42	16.33
5	23 36 38.97	27 18 24.19	8415	m	18.82	18.19	17.90	17.51	17.41	17.02	16.83	16.73	16.68	16.42	16.32	16.26	16.13	16.19
6	23 36 39.00	26 54 35.89	8934	m	18.78	18.04	17.73	17.26	17.12	16.73	16.60	16.49	16.26	16.12	16.00	15.98	15.81	15.79
7	23 36 40.85	26 41 31.50	8738	m	17.90	17.69	17.63	17.48	17.29	17.25	17.21	17.00	17.02	16.92	16.90	16.99	16.85	16.78
8	23 36 42.62	27 17 21.82	...	?	18.11	17.70	17.47	17.24	17.16	16.87	16.75	16.72	16.66	16.52	16.44	16.53	16.45	16.48
9	23 36 43.11	27 13 51.22	17631	b	19.17	18.62	18.20	17.62	17.44	17.05	16.81	16.70	16.56	16.37	16.18	16.15	16.00	15.89
10	23 36 46.45	26 39 47.55	8790	m	17.97	17.74	17.74	17.52	17.29	17.23	17.21	16.93	16.98	16.88	16.84	16.91	16.82	16.62
11	23 36 56.60	27 18 24.42	9869	m	18.82	18.28	18.00	17.66	17.52	17.16	16.96	16.76	16.67	16.49	16.36	16.25	16.14	16.01
12	23 37 00.55	26 49 17.25	31139	b	19.62	19.24	18.82	18.52	18.27	18.07	17.96	17.84	17.65	17.47	17.52	17.42	17.24	17.28
13	23 37 02.10	27 03 42.67	10295	m	17.25	16.91	16.83	16.65	16.59	16.43	16.31	16.04	16.00	16.00	15.91	15.90	15.77	15.74
14	23 37 06.10	26 48 49.80	...	?	19.06	18.64	18.50	18.27	18.04	17.88	17.82	17.66	17.18	17.43	17.30	17.39	17.22	17.03
15	23 37 09.57	26 58 03.12	9477	m	18.57	17.83	17.41	17.01	16.83	16.47	16.28	16.16	16.01	15.82	15.72	15.63	15.46	15.42
16	23 37 13.35	26 54 20.55	9295	m	19.53	18.86	18.56	18.17	17.96	17.63	17.51	17.39	17.21	17.04	16.98	16.90	16.78	16.88
17	23 37 17.30	27 01 09.98	7660	m	13.07	12.64	12.79	11.90	11.36	11.20	11.31	11.15	10.99	11.00	11.14	11.53	11.66	11.67
18	23 37 19.58	26 46 33.00	8892	m	19.19	18.43	18.01	17.63	17.40	17.03	16.99	16.82	16.62	16.44	16.37	16.31	16.14	16.10
19	23 37 20.09	27 08 52.20	9185	m	19.23	18.57	18.11	17.74	17.55	17.25	17.03	16.91	16.73	16.58	16.49	16.36	16.25	16.21
20	23 37 20.23	26 52 42.41	8626	m	17.79	17.04	16.52	16.14	15.92	15.55	15.45	15.25	15.06	14.89	14.78	14.70	14.52	14.45
21	23 37 23.59	27 14 50.53	37924	b	17.11	16.61	16.28	16.07	15.95	15.73	15.60	15.60	15.46	15.40	15.37	15.40	15.35	15.38
22	23 37 25.00	27 03 03.94	10114	m	19.71	19.05	18.83	18.56	18.37	18.17	18.07	17.88	17.63	17.69	17.58	17.52	17.50	17.38
23	23 37 25.86	26 42 45.85	25752	b	17.83	17.98	17.58	17.28	16.86	16.59	16.60	16.28	16.18	16.07	15.89	15.88	15.63	15.62
24	23 37 26.12	27 04 19.35	10075	m	17.97	17.41	17.04	16.66	16.47	16.13	15.92	15.74	15.57	15.44	15.31	15.19	15.06	14.99
25	23 37 27.16	27 04 01.76	9354	m	19.20	18.72	18.32	17.97	17.81	17.52	17.34	17.20	17.05	16.90	16.82	16.71	16.58	16.52
26	23 37 27.38	26 45 04.76	8934	m	18.85	18.56	18.59	18.47	18.28	18.21	18.21	17.97	17.96	17.90	18.05	17.98	17.81	17.63
27	23 37 27.83	26 37 59.56	9790	m	18.04	17.33	16.93	16.53	16.26	15.92	15.87	15.69	15.47	15.35	15.23	15.23	15.06	15.05
28	23 37 30.15	26 46 00.38	7777	m	17.84	17.51	17.41	17.23	17.06	16.88	16.86	16.57	16.57	16.47	16.46	16.47	16.26	16.15
29	23 37 31.69	26 50 15.19	8381	m	18.69	17.92	17.51	17.09	16.88	16.54	16.44	16.30	16.08	15.93	15.82	15.77	15.63	15.58
30	23 37 33.73	27 01 37.11	41327	b	19.69	19.34	18.79	18.24	17.73	17.51	17.22	16.98	16.85	16.67	16.51	16.42	16.24	16.23
31	23 37 35.21	26 48 56.02	35169	b	17.60	17.24	17.16	16.96	16.81	16.64	16.58	16.28	16.31	16.19	16.18	16.14	16.00	15.91
32	23 37 38.11	26 49 10.14	9599	m	19.47	18.87	18.55	18.14	17.91	17.60	17.49	17.37	17.17	17.02	17.00	16.92	16.71	16.76
33	23 37 43.55	27 03 02.98	18425	b	17.29	18.20	17.80	17.59	17.21	16.95	16.97	16.58	16.55	16.56	16.31	16.26	16.11	16.10
34	23 37 44.31	26 42 43.09	...	?	0.00	19.75	19.28	18.91	18.53	18.28	18.15	17.92	17.70	17.48	17.36	17.36	17.15	16.90
35	23 37 46.72	26 58 52.80	11106	m	18.07	17.45	16.95	16.56	16.36	16.03	15.84	15.71	15.54	15.41	15.28	15.17	15.02	14.97
36	23 37 46.97	26 47 00.31	...	?	19.25	18.82	18.39	18.12	17.77	17.59	17.50	17.30	17.10	16.95	16.88	16.89	16.70	16.65
37	23 37 53.75	27 05 18.16	9898	m	19.10	18.47	18.20	17.86	17.69	17.43	17.27	0.00	16.73	16.58	16.59	16.49	16.25	16.21
38	23 37 55.49	27 06 03.67	10187	m	18.62	17.97	17.55	17.15	16.98	16.64	16.45	16.31	16.16	15.99	15.86	15.76	15.62	15.60
39	23 37 56.06	27 11 31.07	37000	b	20.61	21.31	20.91	20.92	20.74	19.98	19.68	19.50	19.42	19.41	18.83	19.15	18.64	18.63
40	23 37 55.75	27 11 14.17	37322	b	19.81	19.40	18.81	18.32	17.84	17.63	17.37	17.10	17.01	16.78	16.63	16.50	16.40	16.39

TABLE 2—*Continued*

No. (1)	R.A. (J2000) (2)	Decl. (J2000) (3)	*cz* (4)	*M* (5)	*b* (6)	*c* (7)	*d* (8)	*e* (9)	*f* (10)	*g* (11)	*h* (12)	*i* (13)	*j* (14)	*k* (15)	*m* (16)	*n* (17)	*o* (18)	*p* (19)
41.....	23 37 56.22	27 04 12.37	18429	b	19.26	18.80	18.20	17.64	17.39	17.10	16.88	16.73	16.54	16.39	16.20	16.16	16.06	15.88
42.....	23 37 56.81	26 54 02.38	25676	b	13.16	12.54	12.75	11.68	11.13	11.00	10.91	11.00	10.56	10.48	10.90	11.04	11.07	11.11
43.....	23 37 57.94	27 15 53.29	10211	m	17.85	17.17	16.73	16.31	16.14	15.75	15.53	15.36	15.24	15.02	14.84	14.73	14.57	14.55
44.....	23 37 58.06	26 57 32.09	...	?	0.00	0.00	20.62	20.23	19.96	19.55	19.51	19.15	18.93	18.57	18.78	18.82	18.42	0.00
45.....	23 37 58.91	27 22 50.69	8721	m	18.14	17.89	17.84	17.71	17.58	17.51	17.36	17.11	17.22	17.12	17.00	17.01	16.92	16.97
46.....	23 37 59.75	26 48 12.50	9410	m	19.57	18.81	18.53	18.22	17.97	17.70	17.60	17.42	17.27	17.12	16.99	17.01	16.88	16.86
47.....	23 38 00.97	26 34 51.51	25915	b	18.48	18.07	17.53	17.12	16.74	16.45	16.43	16.17	15.95	15.81	15.69	15.73	15.58	15.45
48.....	23 38 02.29	26 58 33.82	...	?	0.00	19.48	18.81	18.51	18.36	17.97	17.82	17.74	17.53	17.46	17.47	17.41	17.33	17.26
49.....	23 38 02.32	27 12 10.42	37540	b	19.97	19.37	18.74	18.14	17.65	17.44	17.13	16.92	16.83	16.58	16.44	16.26	16.15	16.10
50.....	23 38 03.13	27 05 23.53	25797	b	20.03	19.68	19.24	18.79	18.65	18.32	18.09	17.96	17.79	17.59	17.43	17.42	17.17	17.30
51.....	23 38 05.02	26 46 11.54	8755	m	18.80	18.25	17.94	17.65	17.36	16.98	16.88	16.59	16.41	16.25	16.16	16.04	15.83	15.75
52.....	23 38 05.05	26 35 55.14	...	?	19.77	19.29	18.92	18.63	18.21	18.05	18.01	17.77	17.62	17.39	17.38	17.40	17.21	17.13
53.....	23 38 06.79	26 44 57.75	10400	m	20.11	19.32	18.86	18.54	18.29	17.95	17.92	17.75	17.53	17.37	17.33	17.36	17.17	17.43
54.....	23 38 09.59	26 55 15.47	9801	m	19.33	18.99	18.60	18.19	17.99	17.67	17.53	17.39	17.20	17.08	17.06	16.89	16.74	16.69
55.....	23 38 10.04	27 12 08.68	7970	m	18.17	18.27	18.25	18.16	17.67	18.09	18.03	17.55	17.89	17.82	17.85	17.84	17.75	0.00
56.....	23 38 10.35	27 01 51.48	8378	m	19.08	18.40	17.98	17.62	17.45	17.11	16.94	16.81	16.64	16.49	16.38	16.29	16.15	16.13
57.....	23 38 11.17	26 37 10.68	...	?	18.73	18.37	18.29	18.16	17.96	17.79	17.82	17.56	17.48	17.44	17.41	17.42	17.33	17.31
58.....	23 38 11.98	26 34 15.69	...	?	19.19	18.72	18.59	18.43	18.26	18.05	18.10	17.91	17.54	17.74	17.64	17.65	17.65	17.48
59.....	23 38 13.79	27 24 52.30	9285	m	17.86	17.11	16.64	16.18	15.99	15.60	15.34	15.18	15.04	14.80	14.65	14.51	14.37	14.32
60.....	23 38 14.40	26 58 03.91	9310	m	19.36	18.75	18.33	17.93	17.78	17.41	17.24	17.12	16.93	16.77	16.70	16.57	16.47	16.43
61.....	23 38 16.17	26 49 03.82	8752	m	17.92	17.21	16.73	16.33	16.11	15.74	15.66	15.50	15.28	15.14	15.07	14.99	14.79	14.80
62.....	23 38 16.33	26 42 22.52	9544	m	0.00	20.10	19.70	19.12	18.58	18.36	18.22	18.01	17.84	17.61	17.62	17.44	17.31	17.32
63.....	23 38 16.76	26 52 05.93	7800	m	18.23	17.95	17.86	17.76	17.56	17.47	17.41	17.12	17.12	17.04	16.97	16.99	16.81	16.70
64.....	23 38 17.28	26 55 42.93	9397	m	18.94	18.24	17.85	17.51	17.31	16.97	16.83	16.68	16.49	16.36	16.29	16.18	16.06	16.04
65.....	23 38 17.76	26 53 18.23	...	?	18.41	17.95	17.55	17.42	17.11	16.81	16.80	16.50	16.50	16.41	16.23	16.05	15.87	15.85
66.....	23 38 18.60	26 53 14.44	9348	m	17.84	17.10	16.59	16.20	15.98	15.60	15.48	15.28	15.09	14.93	14.81	14.70	14.53	14.49
67.....	23 38 18.74	27 02 08.54	9552	m	18.46	17.74	17.23	16.82	16.64	16.26	16.08	15.94	15.71	15.58	15.47	15.33	15.17	15.20
68.....	23 38 19.67	26 42 48.95	...	?	20.02	19.28	18.95	18.56	18.38	18.00	18.00	17.83	17.60	17.46	17.45	17.37	17.25	17.42
69.....	23 38 19.95	26 58 50.25	...	?	19.78	19.41	19.23	19.18	19.00	18.86	18.75	18.82	18.62	18.55	18.90	18.57	18.98	0.00
70.....	23 38 20.85	27 03 04.56	10111	m	18.45	17.75	17.22	16.78	16.61	16.24	16.06	15.90	15.71	15.56	15.42	15.30	15.15	15.11
71.....	23 38 21.44	27 03 02.26	...	?	18.92	18.44	18.04	17.79	17.55	17.25	17.18	16.89	16.85	16.75	16.55	16.46	16.34	16.33
72.....	23 38 21.01	27 18 15.76	9980	m	18.63	17.92	17.45	17.04	16.87	16.51	16.28	16.15	15.99	15.81	15.65	15.57	15.44	15.41
73.....	23 38 22.75	27 12 28.27	8572	m	18.99	18.29	17.84	17.44	17.27	16.93	16.71	16.59	16.42	16.23	16.10	16.02	15.91	15.87
74.....	23 38 22.89	27 09 30.87	9302	m	17.72	17.00	16.51	16.09	15.93	15.56	15.36	15.20	15.04	14.86	14.73	14.61	14.46	14.45
75.....	23 38 22.97	27 17 52.57	37852	b	19.54	19.33	18.87	18.53	18.12	17.94	17.67	17.49	17.39	17.17	17.04	16.96	16.87	16.80
76.....	23 38 25.45	27 01 49.29	9532	m	19.23	18.55	18.15	17.83	17.55	17.19	17.09	16.86	16.75	16.60	16.49	16.33	16.30	16.29
77.....	23 38 26.94	26 59 08.00	10774	m	17.74	17.06	16.55	16.14	15.94	15.57	15.42	15.24	15.07	14.91	14.80	14.66	14.50	14.48
78.....	23 38 26.98	26 43 24.30	...	?	19.42	18.96	18.56	18.31	17.97	17.79	17.71	17.52	17.34	17.12	17.15	17.08	16.92	16.88
79.....	23 38 27.19	27 09 39.10	...	?	19.97	19.33	18.92	18.56	18.34	18.06	17.89	17.75	17.58	17.41	17.34	17.21	17.12	17.20
80.....	23 38 27.25	27 05 27.10	7532	m	18.42	17.76	17.37	16.99	16.85	16.51	16.32	16.19	16.03	15.84	15.74	15.67	15.52	15.50

TABLE 2—*Continued*

No. (1)	R.A. (J2000) (2)	Decl. (J2000) (3)	*cz* (4)	*M* (5)	*b* (6)	*c* (7)	*d* (8)	*e* (9)	*f* (10)	*g* (11)	*h* (12)	*i* (13)	*j* (14)	*k* (15)	*m* (16)	*n* (17)	*o* (18)	*p* (19)
81	23 38 28.72	26 49 08.41	9542	m	17.48	16.76	16.28	15.88	15.66	15.31	15.20	15.05	14.85	14.70	14.61	14.52	14.35	14.39
82	23 38 29.27	27 12 26.32	8403	m	19.86	19.11	18.73	18.34	18.15	17.83	17.62	17.49	17.35	17.15	17.05	16.95	16.84	16.77
83	23 38 29.30	26 58 45.22	9502	m	17.64	16.92	16.40	16.00	15.82	15.43	15.27	15.10	14.94	14.77	14.67	14.52	14.35	14.34
84	23 38 29.36	27 02 25.32	10183	m	19.01	18.49	18.09	17.85	17.53	17.14	17.12	16.80	16.76	16.60	16.45	16.31	16.18	16.17
85	23 38 29.56	27 02 03.32	8104	m	16.69	15.94	15.54	15.25	15.00	14.61	14.54	14.25	14.18	14.01	13.84	13.70	13.49	13.48
86	23 38 29.52	27 01 55.92	9060	m	17.07	16.26	15.74	15.34	15.16	14.78	14.60	14.38	14.22	14.05	13.89	13.79	13.57	13.61
87	23 38 29.36	27 01 51.32	9252	m	16.37	15.53	15.13	14.78	14.54	14.15	14.05	13.78	13.68	13.51	13.34	13.21	13.02	13.01
88	23 38 30.27	26 35 54.52	9395	m	18.42	17.94	17.74	17.52	17.25	17.00	16.99	16.77	16.64	16.52	16.41	16.38	16.28	16.20
89	23 38 31.65	27 21 09.53	9984	m	19.70	19.16	18.81	18.46	18.15	17.86	17.58	17.33	17.22	16.99	16.88	16.73	16.60	16.51
90	23 38 31.69	27 05 42.03	...	?	19.54	18.73	18.10	17.81	17.72	17.33	17.11	17.04	16.90	16.74	16.69	16.75	16.60	16.63
91	23 38 31.36	27 05 40.33	...	?	19.30	18.26	17.86	17.67	17.48	17.09	16.94	16.81	16.70	16.59	16.45	16.54	16.40	16.39
92	23 38 32.33	26 54 36.34	8270	m	18.53	17.90	17.41	17.01	16.84	16.47	16.35	16.20	16.00	15.83	15.78	15.65	15.49	15.52
93	23 38 33.37	27 02 07.05	9828	m	18.25	17.59	17.12	16.71	16.54	16.19	16.01	15.83	15.64	15.48	15.38	15.23	15.05	15.08
94	23 38 34.58	26 58 47.65	8515	m	17.93	17.20	16.66	16.24	16.09	15.71	15.54	15.37	15.19	14.99	14.93	14.78	14.58	14.57
95	23 38 36.16	27 21 01.97	36811	b	19.32	19.01	18.44	17.90	17.41	17.23	16.87	16.69	16.55	16.34	16.24	16.06	15.96	15.99
96	23 38 36.37	27 01 48.37	8378	m	18.02	17.24	16.73	16.31	16.14	15.76	15.58	15.40	15.21	15.02	14.94	14.78	14.60	14.63
97	23 38 37.15	26 43 18.07	5609	f	0.00	19.77	19.39	18.95	18.47	18.30	18.15	17.87	17.68	17.43	17.43	17.30	17.16	17.11
98	23 38 38.91	27 00 42.29	9274	m	17.63	16.87	16.40	15.98	15.80	15.44	15.28	15.10	14.94	14.77	14.68	14.54	14.36	14.39
99	23 38 38.29	27 00 37.38	9356	m	17.81	17.13	16.73	16.44	16.18	15.81	15.73	15.47	15.40	15.23	15.09	14.92	14.75	14.74
100.....	23 38 39.16	27 04 16.69	9443	m	19.02	18.34	17.93	17.53	17.38	17.05	16.88	16.72	16.59	16.41	16.29	16.20	16.04	16.06
101.....	23 38 41.21	26 56 21.20	...	?	19.42	19.06	18.85	18.55	18.31	18.11	17.96	17.77	17.41	17.51	17.39	17.32	17.20	17.07
102.....	23 38 41.85	27 12 56.11	8548	m	18.87	18.24	17.79	17.38	17.20	16.86	16.62	16.49	16.33	16.15	16.04	15.91	15.79	15.74
103.....	23 38 42.18	27 07 08.51	9607	m	18.40	17.69	17.20	16.76	16.58	16.25	16.00	15.86	15.68	15.49	15.37	15.24	15.08	15.06
104.....	23 38 42.43	26 46 25.41	9862	m	16.15	16.41	16.01	15.72	15.42	15.12	15.08	14.80	14.72	14.59	14.42	14.33	14.15	14.14
105.....	23 38 42.77	27 03 27.51	9983	m	19.72	18.97	18.45	18.11	17.92	17.62	17.44	17.27	17.14	16.97	16.84	16.75	16.65	16.62
106.....	23 38 43.23	27 02 32.42	9195	m	19.05	18.31	17.82	17.41	17.25	16.91	16.70	16.57	16.37	16.22	16.12	16.00	15.82	15.89
107.....	23 38 43.77	27 12 56.72	9279	m	17.70	16.96	16.45	16.01	15.82	15.42	15.19	15.00	14.83	14.64	14.50	14.34	14.18	14.16
108.....	23 38 44.32	26 51 04.52	9105	m	18.03	17.29	16.80	16.39	16.16	15.81	15.66	15.49	15.28	15.11	15.04	14.93	14.75	14.74
109.....	23 38 46.24	27 04 48.14	...	?	0.00	19.56	19.14	18.69	18.51	18.24	18.07	17.89	17.72	17.56	17.49	17.34	17.15	17.42
110.....	23 38 46.37	27 10 22.34	9944	m	18.61	17.82	17.34	16.88	16.70	16.33	16.07	15.92	15.75	15.54	15.42	15.29	15.13	15.11
111.....	23 38 48.85	26 35 52.86	12315	m	19.90	19.30	19.01	18.70	18.44	18.23	18.25	18.08	17.78	17.74	17.63	17.68	17.63	0.00
112.....	23 38 48.97	26 55 56.26	...	?	0.00	19.57	19.17	18.77	18.59	18.33	18.13	18.02	17.82	17.66	17.64	17.54	17.39	17.52
113.....	23 38 49.35	27 07 24.26	9066	m	18.46	17.77	17.26	16.84	16.65	16.29	16.03	15.88	15.69	15.49	15.38	15.25	15.08	15.06
114.....	23 38 49.96	26 47 49.16	8029	m	19.14	18.52	18.08	17.75	17.49	17.18	17.05	16.93	16.73	16.57	16.57	16.45	16.28	16.36
115.....	23 38 50.22	27 12 55.47	9139	m	18.09	17.35	16.86	16.44	16.27	15.89	15.66	15.49	15.34	15.13	15.01	14.86	14.72	14.70
116.....	23 38 50.74	27 16 04.77	9272	m	17.30	16.55	16.01	15.57	15.38	15.01	14.76	14.59	14.42	14.21	14.08	13.93	13.78	13.81
117.....	23 38 50.77	27 00 58.47	9970	m	18.69	17.93	17.48	17.11	16.95	16.60	16.41	16.26	16.08	15.94	15.86	15.73	15.57	15.61
118.....	23 38 52.60	26 56 23.58	9059	m	19.13	18.49	18.07	17.73	17.54	17.30	17.02	17.03	16.69	16.54	16.50	16.38	16.23	16.22
119.....	23 38 53.12	27 02 02.09	9940	m	0.00	19.61	19.18	18.78	18.54	18.27	18.07	17.93	17.77	17.56	17.50	17.40	17.28	17.37
120.....	23 38 54.05	27 02 45.89	9643	m	18.58	17.89	17.39	16.99	16.83	16.49	16.28	16.14	15.94	15.77	15.67	15.56	15.39	15.44

TABLE 2—*Continued*

No. (1)	R.A. (J2000) (2)	Decl. (J2000) (3)	*cz* (4)	*M* (5)	*b* (6)	*c* (7)	*d* (8)	*e* (9)	*f* (10)	*g* (11)	*h* (12)	*i* (13)	*j* (14)	*k* (15)	*m* (16)	*n* (17)	*o* (18)	*p* (19)
121.....	23 38 53.72	27 02 39.49	9435	m	18.40	17.79	17.39	17.06	16.86	16.52	16.40	16.19	16.06	15.91	15.79	15.69	15.60	15.59
122.....	23 38 54.17	27 04 18.49	...	?	19.07	18.43	17.92	17.52	17.35	17.03	16.83	16.67	16.49	16.30	16.21	16.11	15.97	15.99
123.....	23 38 55.29	26 50 38.10	38628	b	0.00	19.67	19.07	18.56	17.96	17.80	17.54	17.29	17.16	16.92	16.87	16.70	16.57	16.59
124.....	23 38 55.55	26 51 19.50	10283	m	19.55	18.89	18.49	18.10	17.56	17.30	17.12	16.79	16.65	16.48	16.29	16.17	16.11	16.10
125.....	23 38 56.35	27 09 43.01	9276	m	18.16	17.44	16.91	16.49	16.32	15.96	15.74	15.59	15.43	15.21	15.12	14.98	14.82	14.83
126.....	23 38 56.50	26 56 56.61	9216	m	19.48	18.86	18.47	18.12	17.92	17.66	17.48	17.33	17.14	16.98	16.91	16.83	16.65	16.62
127.....	23 38 58.86	27 15 20.23	8666	m	19.28	18.63	18.15	17.73	17.54	17.22	16.97	16.83	16.67	16.46	16.41	16.24	16.11	16.17
128.....	23 39 01.53	27 13 00.65	9032	m	19.61	18.97	18.55	18.16	18.03	17.66	17.46	17.25	17.17	16.99	16.82	16.73	16.60	16.63
129.....	23 39 01.61	26 57 32.55	9056	m	19.11	18.38	17.90	17.49	17.32	17.02	16.82	16.68	16.51	16.32	16.26	16.17	16.00	15.98
130.....	23 39 01.61	26 33 56.55	10542	m	0.00	17.10	16.70	16.34	16.05	15.69	15.67	15.42	15.29	15.18	15.01	14.93	14.74	14.73
131.....	23 39 01.63	27 18 01.15	9832	m	18.92	18.19	17.75	17.32	17.11	16.79	16.55	16.38	16.24	15.97	15.85	15.75	15.61	15.58
132.....	23 39 01.91	27 13 26.05	10488	m	18.48	17.87	17.34	16.92	16.79	16.38	16.16	15.97	15.88	15.64	15.47	15.39	15.23	15.25
133.....	23 39 02.63	27 06 09.55	10144	m	17.49	16.90	16.50	16.18	15.94	15.52	15.43	15.16	15.10	14.89	14.69	14.59	14.41	14.40
134.....	23 39 05.23	27 12 40.17	...	?	19.00	18.08	17.35	17.08	16.89	16.46	16.25	16.10	15.96	15.81	15.73	15.71	15.72	15.64
135.....	23 39 06.99	27 00 37.78	8898	m	19.62	18.91	18.53	18.11	17.93	17.64	17.47	17.30	17.10	16.96	16.82	16.78	16.64	16.69
136.....	23 39 07.01	26 38 05.88	11685	m	19.31	19.09	18.93	18.86	18.53	18.50	18.58	18.28	18.17	18.14	18.16	18.12	18.08	0.00
137.....	23 39 07.16	26 53 17.39	8762	m	19.47	18.78	18.34	17.93	17.73	17.41	17.29	17.10	16.94	16.75	16.71	16.59	16.47	16.49
138.....	23 39 07.17	27 12 22.09	9751	m	18.86	18.17	17.73	17.27	17.11	16.78	16.55	16.39	16.23	16.03	15.91	15.80	15.69	15.65
139.....	23 39 09.12	27 24 13.50	8697	m	17.65	17.13	16.67	16.25	16.17	16.05	15.60	15.66	15.42	15.23	15.17	15.19	15.12	15.18
140.....	23 39 09.38	27 18 27.60	7577	m	18.78	18.17	17.81	17.45	17.24	16.98	16.75	16.54	16.45	16.25	16.18	16.07	15.94	15.87
141.....	23 39 09.89	26 41 37.61	8149	m	18.54	18.18	18.03	17.75	17.58	17.36	17.34	17.13	17.01	16.89	16.88	16.86	16.72	16.86
142.....	23 39 10.45	26 50 44.51	9381	m	19.76	19.25	18.86	18.34	18.12	17.82	17.68	17.55	17.35	17.19	17.14	17.06	16.94	16.79
143.....	23 39 12.02	27 06 56.52	7608	m	17.92	17.23	16.82	16.44	16.21	15.85	15.65	15.41	15.21	15.05	14.93	14.82	14.65	14.61
144.....	23 39 12.03	27 09 37.32	7919	m	18.78	18.10	17.65	17.24	17.04	16.70	16.46	16.24	16.05	15.85	15.76	15.61	15.48	15.40
145.....	23 39 14.02	26 37 23.43	9716	m	14.63	14.18	13.95	13.76	13.58	13.40	13.44	13.38	13.19	13.12	13.19	13.29	13.15	13.30
146.....	23 39 17.42	26 57 50.36	8129	m	18.23	18.16	18.08	18.00	17.83	17.90	17.81	17.47	17.60	17.60	17.58	17.59	17.48	17.32
147.....	23 39 17.99	26 50 42.36	8002	m	17.85	17.49	17.32	17.13	16.94	16.84	16.74	16.57	16.46	16.38	16.38	16.36	16.21	16.25
148.....	23 39 19.17	27 14 45.97	9639	m	18.23	17.52	17.01	16.59	16.36	16.02	15.75	15.58	15.39	15.21	15.08	14.94	14.77	14.74
149.....	23 39 20.70	26 45 11.78	9424	m	18.38	17.61	17.16	16.74	16.50	16.15	16.06	15.88	15.68	15.52	15.45	15.37	15.20	15.21
150.....	23 39 25.75	27 22 36.42	17120	b	0.00	19.73	19.18	18.55	18.30	18.08	17.71	17.61	17.42	17.21	17.10	16.99	16.86	16.86
151.....	23 39 27.52	27 03 49.23	9710	m	19.78	18.99	18.61	18.21	17.99	17.73	17.49	17.37	17.19	17.03	16.92	16.84	16.72	16.65
152.....	23 39 28.55	27 17 50.94	9310	m	19.21	18.71	18.23	17.79	17.56	17.28	17.00	16.84	16.72	16.48	16.39	16.23	16.13	16.09
153.....	23 39 30.77	27 01 56.85	8828	m	18.75	18.06	17.60	17.17	16.97	16.65	16.43	16.27	16.09	15.91	15.80	15.70	15.52	15.56
154.....	23 39 33.78	26 52 15.37	8802	m	0.00	19.27	18.80	18.44	18.17	17.89	17.77	17.60	17.45	17.27	17.24	17.06	16.95	16.86
155.....	23 39 33.80	27 09 58.17	9375	m	19.18	18.41	17.91	17.43	17.21	16.86	16.63	16.42	16.25	16.05	15.93	15.79	15.64	15.59
156.....	23 39 34.05	27 19 53.07	10138	m	19.74	19.08	18.64	18.16	17.96	17.69	17.39	17.23	17.10	16.89	16.77	16.66	16.56	16.61
157.....	23 39 34.53	26 53 41.08	11749	m	0.00	0.00	18.36	18.11	17.88	17.73	17.62	17.35	17.28	17.21	17.10	17.04	16.92	16.92
158.....	23 39 34.73	27 27 06.28	37981	b	0.00	20.04	19.30	18.74	18.24	18.11	17.64	17.39	17.25	16.97	16.91	16.69	16.57	16.55
159.....	23 39 37.87	27 08 51.00	9728	m	19.71	18.98	18.43	17.96	17.74	17.42	17.18	16.98	16.79	16.61	16.51	16.34	16.22	16.19
160.....	23 39 46.22	26 41 21.46	7945	m	18.58	18.06	17.90	17.63	17.43	17.24	17.16	17.05	16.93	16.79	16.76	16.77	16.63	16.58

TABLE 2—*Continued*

No. (1)	R.A. (J2000) (2)	Decl. (J2000) (3)	*cz* (4)	*M* (5)	*b* (6)	*c* (7)	*d* (8)	*e* (9)	*f* (10)	*g* (11)	*h* (12)	*i* (13)	*j* (14)	*k* (15)	*m* (16)	*n* (17)	*o* (18)	*p* (19)
161.....	23 39 49.54	27 22 35.08	9958	m	17.82	17.15	16.67	16.12	15.88	15.59	15.26	15.07	14.96	14.70	14.54	14.40	14.26	14.25
162.....	23 39 49.95	26 59 32.88	...	?	19.83	19.31	18.97	18.53	18.30	18.11	17.90	17.77	17.62	17.43	17.38	17.35	17.22	17.33
163.....	23 39 54.88	26 57 35.62	...	?	19.35	18.87	18.64	18.32	18.08	17.99	17.73	17.60	17.46	17.34	17.31	17.19	17.14	17.14
164.....	23 39 55.20	26 40 29.02	8686	m	18.84	18.17	17.79	17.32	17.06	16.72	16.61	16.42	16.28	16.07	16.00	15.93	15.75	15.83
165.....	23 39 58.51	26 50 02.94	8659	m	16.80	16.39	15.99	15.68	15.41	15.01	14.90	14.67	14.55	14.40	14.21	14.13	13.93	13.92
166.....	23 40 00.95	27 08 01.46	9398	m	17.07	16.35	15.80	15.31	15.09	14.71	14.45	14.24	14.10	13.90	13.75	13.63	13.44	13.42
167.....	23 40 03.33	27 10 02.67	8347	m	18.34	17.70	17.15	16.65	16.47	16.14	15.87	15.69	15.56	15.32	15.20	15.10	14.94	14.93
168.....	23 40 04.34	27 08 03.58	9985	m	19.07	18.45	17.95	17.44	17.24	16.91	16.62	16.47	16.28	16.10	15.96	15.84	15.72	15.70
169.....	23 40 04.43	26 48 58.98	...	?	15.92	17.63	17.23	17.53	16.89	16.87	16.67	16.62	16.44	16.23	16.21	16.42	16.03	16.02
170.....	23 40 05.48	27 11 20.49	9564	m	18.59	17.96	17.46	16.88	16.69	16.40	16.09	15.92	15.75	15.54	15.41	15.31	15.15	15.10
171.....	23 40 08.69	26 54 03.11	...	?	18.19	17.65	17.26	16.95	16.74	16.53	16.42	16.29	16.18	16.10	16.08	16.11	16.01	16.07
172.....	23 40 11.15	27 25 45.62	...	?	19.00	18.54	18.10	17.44	17.30	17.08	16.64	16.49	16.37	16.17	16.04	15.93	15.87	15.87
173.....	23 40 12.08	26 54 24.53	19322	b	19.80	19.33	18.89	18.29	18.03	17.74	17.54	17.37	17.17	17.03	16.85	16.87	16.72	16.58
174.....	23 40 12.66	27 20 05.93	20884	b	19.91	19.61	19.12	18.48	18.22	18.00	17.64	17.46	17.11	17.05	16.88	16.85	16.89	16.60
175.....	23 40 13.20	27 18 26.04	...	?	18.72	18.46	18.24	17.87	17.73	17.57	17.32	17.09	17.01	16.88	16.78	16.73	16.62	16.57
176.....	23 40 13.83	26 51 39.34	...	?	18.39	18.03	17.82	17.50	17.32	17.23	17.10	16.95	16.50	16.73	16.58	16.67	16.56	16.43
177.....	23 40 22.22	27 11 05.70	10047	m	18.53	17.88	17.43	16.85	16.68	16.40	16.07	15.94	15.74	15.56	15.41	15.29	15.17	15.14
178.....	23 40 23.18	27 02 15.40	...	?	19.33	18.81	18.64	18.29	18.14	18.01	17.76	17.62	17.45	17.40	17.31	17.37	17.21	17.16

NOTE.—Units of right ascension are hours, minutes, and seconds, and units of declination are degrees, arcminutes, and arcseconds.

for each filter band are larger at fainter depths. Typically, the errors are 0.02 mag for bright stars (say, $m < 16.5$ mag) and 0.05 mag at $m = 19.0$ mag.

For magnitudes in the *c* and *o* filters, the errors from the model calibration (Zhou et al. 1999) should be taken into account. By comparing the observed SEDs and the template SEDs, the typical errors are 0.05 and 0.10 mag, respectively, for the *c* and *o* filters, which should be larger than the upper limits of the observational errors because the difference between observed SEDs and template SEDs includes observational measurements errors, template SED errors, and data-fitting errors. The principle of this kind of error estimation can be found in Zhou et al. (2001).

3. ANALYSES OF THE SEDs OF THE KNOWN MEMBER GALAXIES

3.1. *Sample of 124 Known Member Galaxies*

In general, it is not reasonable to select all the member galaxies in a nearby cluster by simply setting two fixed velocity limits because the dispersion of line-of-sight velocities of members is expected to be larger in the inner region of the cluster and smaller in the outer region, whether the cluster is gravitationally bound and isolated or whether there exists a significant amount of secondary infall. The velocity dispersion as a function of angular separation for all galaxies within central 6° region of Abell 2634 was calculated by SSGH (see Fig. 5 in SSGH).

Since our observations focus on only 0.95 deg^2 centered on Abell 2634, it is reasonable to select member galaxies within our field by the criterion of 7000 km s^{-1} < cz < 13,000 km s^{-1}. The velocity dispersion in central region of Abell 2634 should be larger, and a negligible contamination of galaxies in Abell 2666 (with 3° angular separation) can be expected. Among 178 known galaxies, there are 147 galaxies having redshift information, including 124 member galaxies (i.e., 7000 km s^{-1} < cz < 13,000 km s^{-1}), 22 background galaxies (i.e., cz > 13,000 km s^{-1}), and one foreground galaxy (i.e., cz < 7000 km s^{-1}). A check of our list of member galaxies with those in SSGH shows that all galaxies in the HDR sample are found to be included. Figure 1 shows the distribution of all galaxies with known redshifts in our field. Some galaxies not belonging to Abell 2634 are found in our field, including seven galaxies belonging to a rich cluster, Abell 2622, centered at 0.°9 to the northeast of Abell 2634 and 10 galaxies belonging to a background cluster that is almost behind the center of Abell 2634. One galaxy with a redshift of 5609 km s^{-1} should belong to the foreground branch of the PPS (Pinkney et al. 1993). It is easy to see that the highest peak occurs at ~9300 km s^{-1}, which is associated with Abell 2634.

3.2. *Comparison between SED Templates and Observed SEDs*

In order to check the reliability of our SEDs, it is interesting and important to compare the SEDs of the 124 member galaxies with the template SEDs. To obtain the template SEDs for all types of galaxies, we shifted the original galaxy library spectra (Kinney et al. 1996) with a redshift of $z = 0.03$, the mean redshift of Abell 2634, and then convolved them with the filter transmission curves of the BATC filter system. The majority of galaxies in the central region are early-type galaxies (i.e., E and S0). To form a sample of early-type member galaxies, we searched the morphological information in the Principle Catalog of Galaxies (1999 version) in the Lyon-Meudon Extragalactic Database (Paturel et al. 1997). Then, we checked and supplemented the list, referring to some recent literature (Scodeggio, Giovanelli, & Haynes 1998; Lucey et al. 1997; Scodeggio, Giovanelli, Haynes 1997; Pinkey et al. 1993; Lucey et al. 1991). As a result, 60 early-type galaxies (E and S0), two S0a galaxies, nine spiral galaxies, and one irregular galaxy were found in our sample. Note that it is difficult to separate lenticular galaxies from elliptical galaxies from the previous imaging and spectroscopic observations. That is why the morphological indices given in the literature for a certain number of early-type galaxies are quite diverse and inconsistent. Furthermore, the template SEDs of our BATC filter

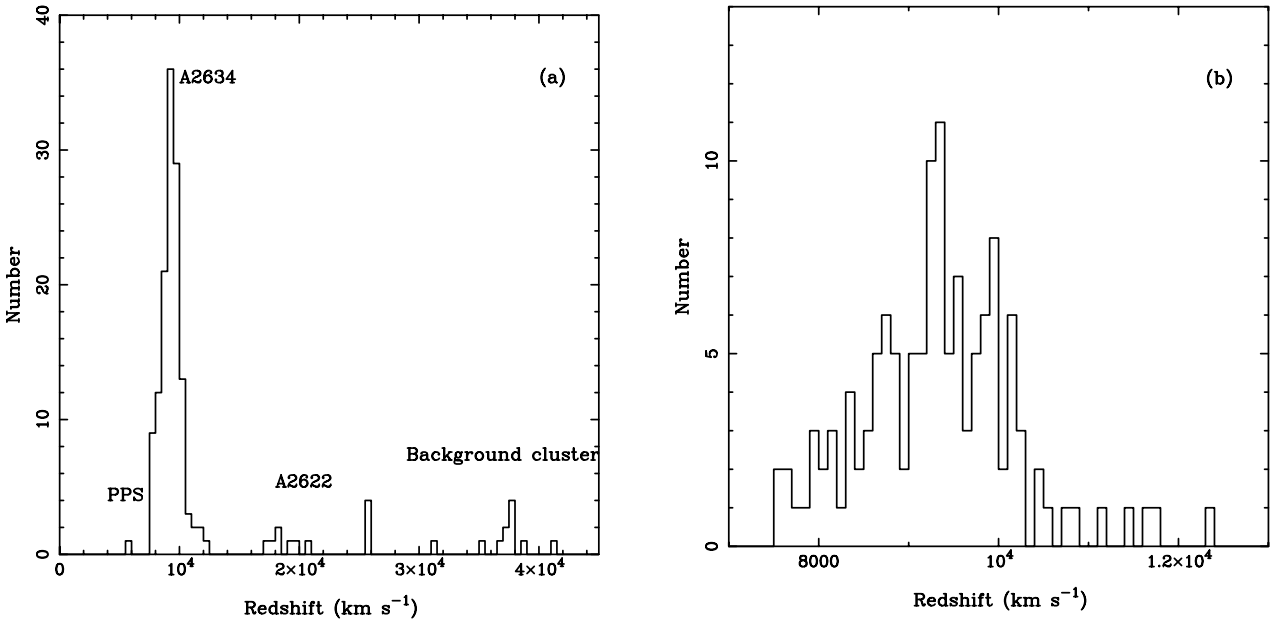

FIG. 1.—Histograms of redshifts, cz, of known galaxies in our field for (*a*) 147 known galaxies and (*b*) 124 member galaxies. The bin widths are 500 and 100 km s^{-1}, respectively.

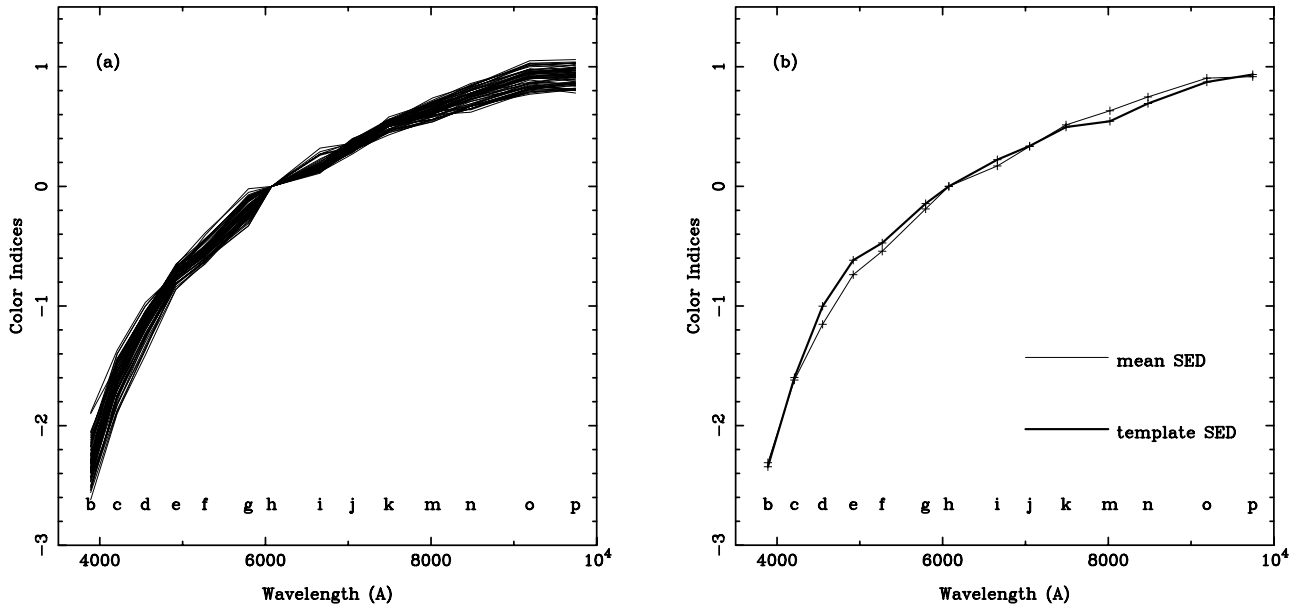

FIG. 2.—(*a*) SEDs of 59 early-type galaxies. The mean and template SEDs are plotted in (*b*) with thin and thick lines, respectively.

system for elliptical and lenticular galaxies are found to be almost identical. We shall analyze the SED features of early-type galaxies, including E and S0, as a whole in the current study.

The SEDs of 60 early-type galaxies with reference to the magnitude in the *h* band are shown in Figure 2*a*. We find that their SEDs are quite similar. The negligible SED dispersion is rather reasonable, which should be mainly due to the slight deviation of their redshifts and stellar metallicities. The mean SED of our sample has a better fit to the SED template, which can be seen in Figure 2*b*.

We find that many observed SEDs of galaxies are very similar to the template spectra. As an example, Figure 3 show the SED of the central galaxy, NGC 7720, and the template spectrum of elliptical galaxies.

3.3. *Verification of Color-Magnitude Relation*

Our multicolor photometric observations allow a verification of the so-called color-magnitude relation. Many previous studies showed that fainter early-type galaxies tend to have colors bluer than the brighter galaxies do (see Bower et al. 1992, and references therein). In other words, there should be a correlation for the early-type galaxies between their colors and absolute magnitudes. For the members of a galaxy cluster, the differences in apparent magnitudes can well reflect the differences in absolute luminosities.

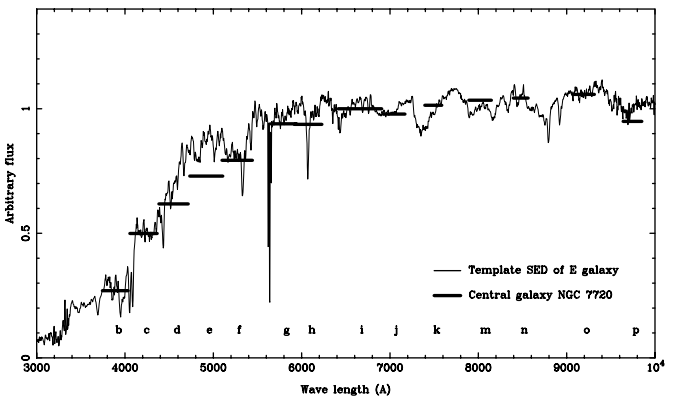

FIG. 3.—SED of the central galaxy NGC 7720 and the template spectrum of the elliptical galaxy.

Figure 4 shows plots of two color indices (C.I.'s), mag(3890 Å)−mag(9745 Å) and mag(4210 Å)−mag(9190 Å), versus mag(6075 Å) for all known member galaxies in the central region of Abell 2634. For 60 early-type galaxies, there exists a clear correlation between color and brightness, in the sense that the brighter galaxies are redder, which is known as the color-magnitude effect. This effect is comparatively remarkable for color mag(3890 Å)−mag(9745 Å) (in Fig. 4*a*), with a linear fit of C.I. $= -0.16(\pm 0.03)m_h + 5.70(\pm 0.48)$. The correlation coefficient is 0.58, and the rms dispersion is 0.17. The error on the intercept does not take into account the error on the slope. The color index, mag(4210 Å)−mag(9190 Å), also shows such a correlation, with a linear fit of C.I. $= -0.12(\pm 0.03)m_h + 4.43(\pm 0.43)$, which is shown in Figure 4*b*. Its corresponding correlation coefficient is 0.52, and the rms dispersion is 0.15. The linear fits are plotted as solid lines, and the dashed lines in panels (*a*) and (*b*) represent $\sigma_{\text{C.I.}} = 0.48$ and 0.43, respectively.

The elliptical galaxies in the Virgo and Coma clusters are found to have a tighter color-magnitude correlation than lenticular galaxies do (Bower et al. 1992). However, as mentioned above, we cannot accurately separate elliptical galaxies from lenticular galaxies in our sample. The lenticular galaxies in our sample might contribute considerably to the dispersion of the color-magnitude relation. For the sake of comparison, the late-type galaxies and the remaining members without morphological information are also plotted. It is evident that late-type galaxies do not obey such a correlation, and some galaxies with unknown morphologies have color indices significantly different than the correlation, similar to some spiral galaxies.

To understand the color-magnitude relation, the SEDs of three member elliptical galaxies with considerably different magnitudes are shown in Figure 5. The reddening of bright galaxies occurs mainly in the violet region shortward of 4250 Å, corresponding to the wavelength domain of filters *b*

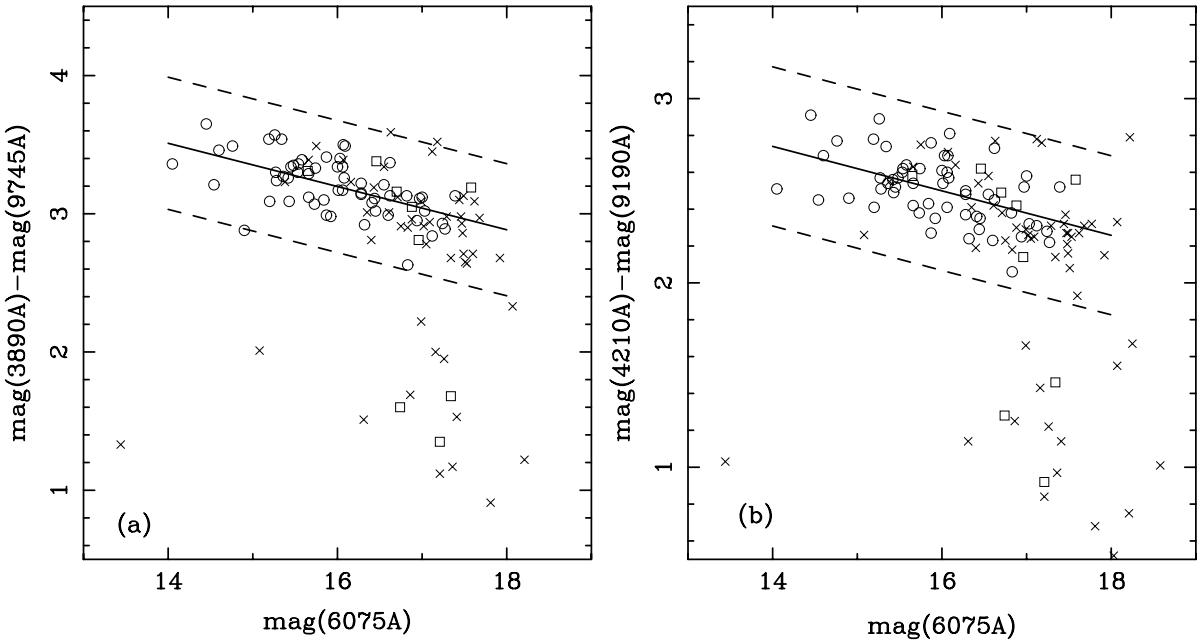

FIG. 4.—Color-magnitude effect for early-type galaxies (*open circles*) in the central region of Abell 2634. (*a*) The color-magnitude relation for the color index mag(3890Å)− mag(9745Å) and (*b*) that for color index mag(4210Å)−mag(9190Å). The colors of the known spiral galaxies and the galaxies with unknown morphologies are denoted by open squares and crosses, respectively. The linear fits are plotted as solid lines, and the dashed lines in (*a*) and (*b*) represent $\sigma_{\rm C.I.} = 0.48$ and 0.43, respectively.

and *c*, where stellar spectra are richest in metal absorption lines and the SEDs turn to be rather steep. It has been well demonstrated that the BATC filter system has a great advantage for studying this effect. The filters *b* and *c* have bandwidths of ~300 Å centered on 3890 and 4210 Å, and the wavelengths of filters *p* and *o* reach longward of 9000 Å. The color-magnitude correlation can be used to analyze the membership possibility of the faint objects within our observational field.

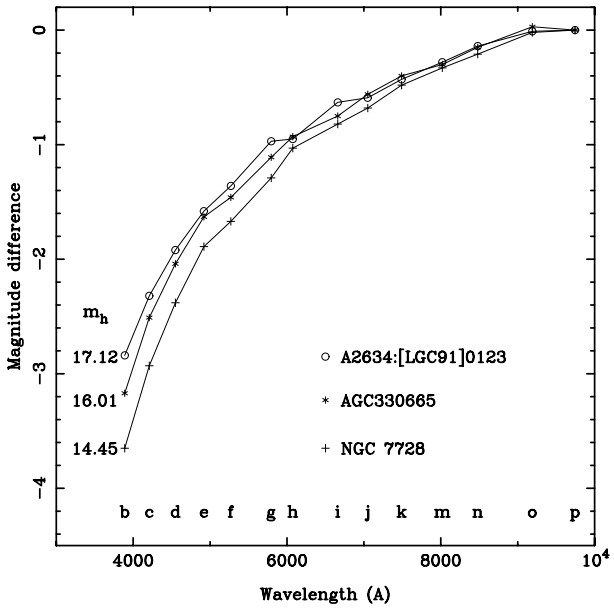

FIG. 5.—SEDs of three member elliptical galaxies with considerably different magnitudes. The *h* magnitudes and names of these elliptical galaxies are also given.

3.4. *Test of the Technique of Photometric Redshift*

It is well known that the technique of photometric redshifts can be used to estimate the redshifts of galaxies by using the SED information from the multicolor photometric observations. Particularly with the development of large and deep field surveys, this technique has been extensively applied (Lanzetta, Yahil, & Fernández-Soto 1996; Arnouts et al. 1999; Furusawa et al. 2000). The photometric redshift of a given object, $z_{\rm phot}$, corresponds to the best fit of its photometric SED by the set of template spectra. We also developed some procedures for estimating the photometric redshifts, especially for the multicolor photometric observations by the BATC filter system (Huang et al. 2001), based on the standard SED-fitting code called HYPERZ (Bolzonella, Miralles, & Pelló 2000). It is crucial to test the reliability in all cases by comparison between the photometric and the spectroscopic redshifts, using the sample of relatively bright objects.

The photometric redshift technique is traditionally used to search for galaxies or AGNs with comparatively high redshifts. The accuracy of photometric redshift is heavily dependent upon the photometric accuracy. Our sample of 124 member galaxies allows an opportunity to check our photometric accuracy and to test whether our SED-fitting procedures are sensitive for estimating the redshifts of nearby bright galaxies. Thanks to the large number of filters, from *b* (close to the traditional *U* filter) to *p* (near-IR) bands, the accuracy of $z_{\rm phot}$ estimates is expected to be improved. In this calculation, we only use the SED templates of normal galaxies, and the reddening law with a $A_V \sim 0.3$ is taken from Calzetti et al. (2000). The searching step of redshifts is 0.005. The comparisons between the $z_{\rm phot}$ and spectroscopic redshift ($z_{\rm sp}$) for 124 known member galaxies are shown in Figure 6. The dotted line corresponds to $z_{\rm phot} = z_{\rm sp}$, and the error bar in the $z_{\rm phot}$ determination at

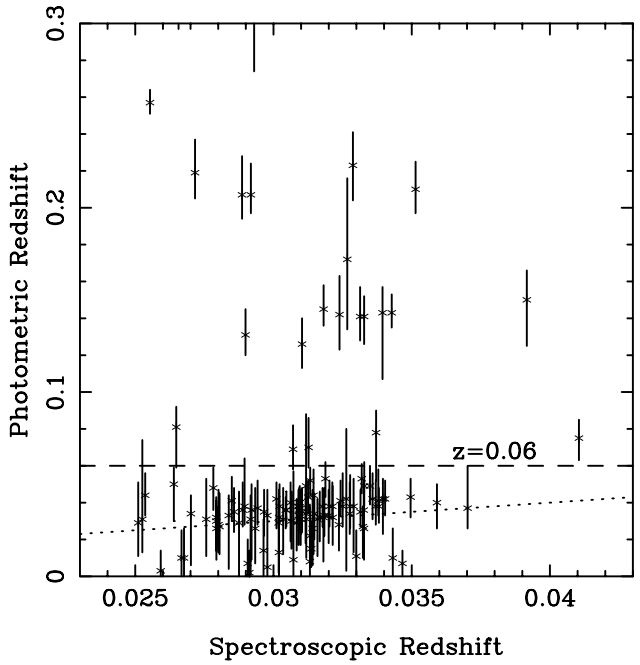

FIG. 6.—Comparison between the photometric redshift (z_{phot}) and spectroscopic redshift (z_{sp}) for 124 known member galaxies. The dotted line corresponds to $z_{phot} = z_{sp}$, and the error bar in the z_{phot} determination at 68% confidence level is also given.

68% confidence level is also given. It is obvious that the majority (98/124) of the member galaxies are found to have $z_{phot} < 0.06$; there is a dense group at $z_{phot} \sim 0.031$, the exact redshift of Abell 2634. Some galaxies with larger deviations are likely to have peculiar features in reddening and metallicity evolution. The results demonstrate that our SED-fitting procedures are quite efficient in photometric redshift estimation for galaxies belonging to such a nearby cluster. After a careful star-galaxy separation for all objects detected, we will apply in the following section the technique of photometric redshift to the faint galaxies for selecting the faint galaxies probably belonging to Abell 2634.

The morphological information is also provided by the SED-fitting procedures. If we just classify member galaxies into early and late types, the classification by the SED-fitting technique is quite accurate for the early types. Among 60 known early-type members, only three early types are incorrectly classified as the late types. On the other hand, the misclassification rate for the late-type galaxies is comparatively high, five of nine spiral galaxies are misclassified as early types. As a result, it is likely to include more elliptical galaxies for our SED-fitting procedures. For the remaining 52 known members without morphological information in the literature, we shall take the classification given by our SED-fitting procedures in the following analyses.

4. SELECTION OF FAINT MEMBER GALAXIES OF ABELL 2634

4.1. *Star-Galaxy Separation*

There are 5572 objects detected by our photometric measurements, and most of them should be faint stars. We know that the spectra of stars are significantly different from type to type, and they are also distinct from those of galaxies. It should be easy to separate galaxies from the whole list of faint sources based on the SED information.

Generally, the color-color diagram is a powerful tool because different objects with distinct color indices usually occupy different regions in the diagram. Figure 7 shows four types of color-color diagrams that we will use in further star-galaxy separation. These diagrams include the following categories of objects: (1) all types of stars in our SED template library (denoted by asterisks), (2) morphologically various galaxies with template SEDs (denoted by open circles), (3) the known member galaxies in our field (denoted by crosses), and (4) all the remaining objects detected by our photometric measurements (denoted by dots). The most striking feature is that the stars in our SED template library lie in a well-defined band stretching from top left to bottom right, with which the majority of objects detected in our observations are associated. This band is a color sequence, with the bluer (early-type) stars at the top left and the redder (late-type) stars at the bottom right, in the similar sense of the main sequence in H-R diagram. However, the known galaxies are distributed in a region just above the band, and the objects in a relatively dense region ("barlike") are populated by most early-type (E, S0) member galaxies. The dashed lines in Figure 7 can be used to set the limits between stars and galaxies.

The color-color diagram in Figure 7*a* is the best tool to distinguish galaxies in our SED catalog. The magnitudes in the *h* filter (6075 Å) are available for the majority of the sources detected. The numbers of objects detected in the *b* (3890 Å) and *p* bands (9745 Å) are relatively small, mainly because of the low intrinsic fluxes in these two bands. A certain number of objects in our SED list are found to have not been detected in the *b* and/or *p* bands, for which we cannot use the diagram in Figure 7*a* to perform star-galaxy separation. Alternatively, the magnitudes in *c* (4210 Å) and *o* (9190 Å) bands can be used for star-galaxy separation.

In practice, we excluded all the known galaxies from the list of 5573 objects and then divided the remaining objects into following four categories: (1) 1157 objects with *b*, *h*, and *p* magnitudes; (2) 122 objects with *b*, *h*, and *o* magnitudes, but without *p* magnitude; (3) 401 objects with *c*, *h*, and *p* magnitudes, but without *b* magnitude; (4) 220 objects with *c*, *h*, and *o* magnitudes, but without *b* and *p* magnitudes. It is appropriate for these four categories to produce the star-galaxy separations by those four color-color diagrams given in Figure 7. As a result, we obtained 359 faint galaxies in our field; the technique of photometric redshift will be applied for membership selection to those in the following section.

4.2. *Membership Selection by Photometric Redshift Estimation and Color-Magnitude Correlation*

The results of the application of the photometric redshift technique on the 124 known member galaxies opened a straight way for membership selection. To produce the list of faint member galaxies, we applied the technique of photometric redshift upon 359 faint galaxy candidates. We chose the same parameters in the testing application except taking a smaller step of photometric redshift, 0.002 (i.e., 600 km s^{-1}). The histogram of estimated photometric redshifts is shown in Figure 8. Most of candidates are found to have z_{phot} less than 0.25. A certain fraction of galaxies lie in the bump within a region of z_{phot} from 0.0 to 0.06, corresponding to a radial velocity limit of $V_r < 18{,}000$ km s^{-1}. About

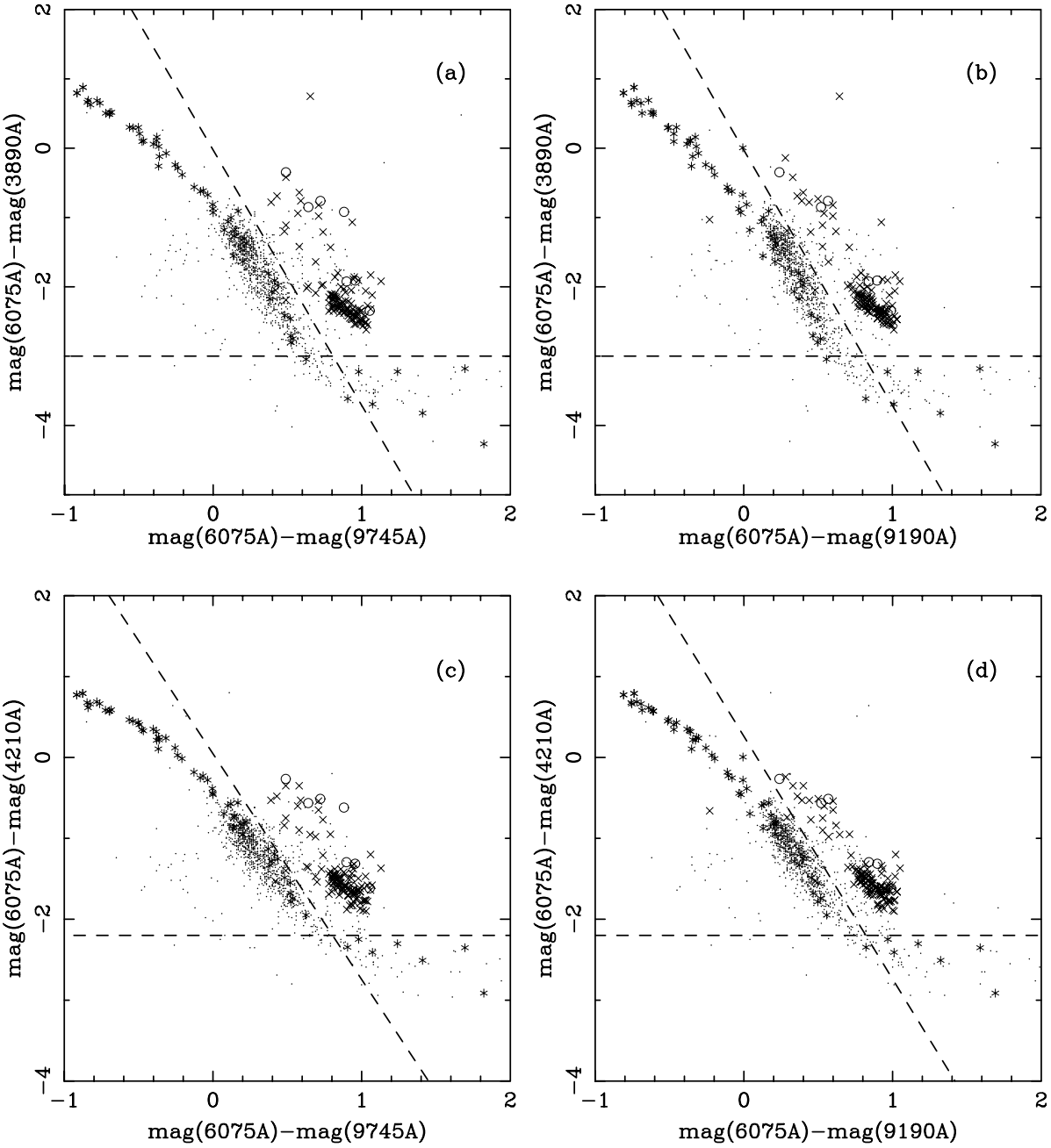

FIG. 7.—Four kinds of color-color diagrams used in our star-galaxy separation. The color indices of symbols in the diagrams distinguish the galaxies as follows: asterisks for all types of stars in our SED template library, open circles for morphologically different galaxies with template SEDs, crosses for the known member galaxies in our field, and the minor dots for all the objects detected in the b/c and o/p bands by our photometric measurements.

80% of the known galaxies were computed to have the photometric redshifts within this $z_{\rm phot}$ region (see Fig. 6). Therefore, we adopt 0.06 as the limit between members and nonmembers, and 76 galaxies are selected to be member candidates.

Among the 76 member candidates, 68 (90%) galaxies are detected as early-type galaxies by our SED-fitting procedures, including 60 E and eight S0 galaxies. The testing application on the 124 known members shows that some late-type galaxies, particularly for Sa galaxies, are likely to be misclassified as early types. For these 68 early-type member candidates, a further selection by color-magnitude correlation is performed. Figure 9 gives the color-magnitude diagram for all 359 galaxy candidates, including 68 newly selected member candidates (denoted by circled dots). We find that a majority of early-type member candidates obey the previous form of color-magnitude relation that is derived only by bright early-type galaxies. There are 10 candidates with colors beyond the 2 σ deviation of intercept that have probably been misclassified. Taking only the templates of late-type galaxies, we applied the SED-fitting procedures again on these 10 member candidates. As a result, 8 of the 10 galaxies are found to have redshifts less than 0.06, with the best fit to the template SEDs of Sa or Sb galaxies, and they are therefore regarded as late-type member galaxies. The remaining two galaxies with larger photometric redshifts are excluded.

Finally, 74 galaxies (including 58 early-types and 16 spiral galaxies) are selected as faint member galaxies in the central region of Abell 2634. The SED information for these

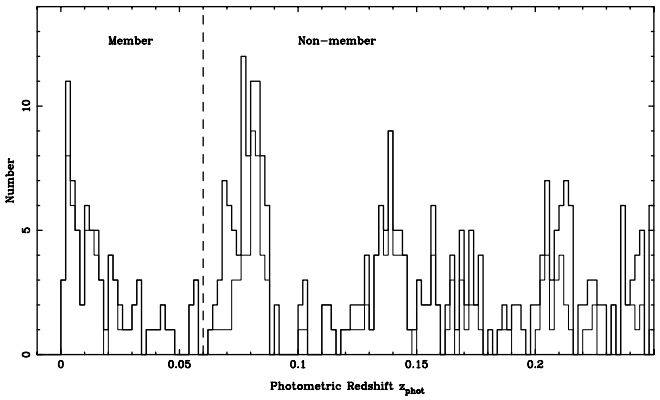

FIG. 8.—Distribution of photometric redshifts for 359 faint galaxies (*thick line*). The redshift of 0.06 is adopted as the limit between members and nonmembers. The thin line corresponds to the z_{phot} distribution of early-type galaxies.

74 faint members is cataloged in Table 3, as well as their positions, z_{phot} values, and morphological classes T (E, S0, Sa, and Sb galaxies are represented by 1, 2, 3, and 4, respectively).

5. SPATIAL AND COLOR PROPERTIES OF OUR ENLARGED SAMPLE

Combining with the 124 known member galaxies, we achieved a larger sample of members in the central region of Abell 2634. Statistically, there are 198 member galaxies, including 160 early types (102 E, 56 S0, and two S0a) and 37 late types (13 Sa, 18 Sb, and six Sc), taking the morphological classification given by our SED-fitting procedures for 52 known members without morphological information in the literature.

Based on the enlarged sample of member galaxies, we can observe the spatial distribution in the central region of Abell 2634. Figure 10 gives the spatial distribution of all

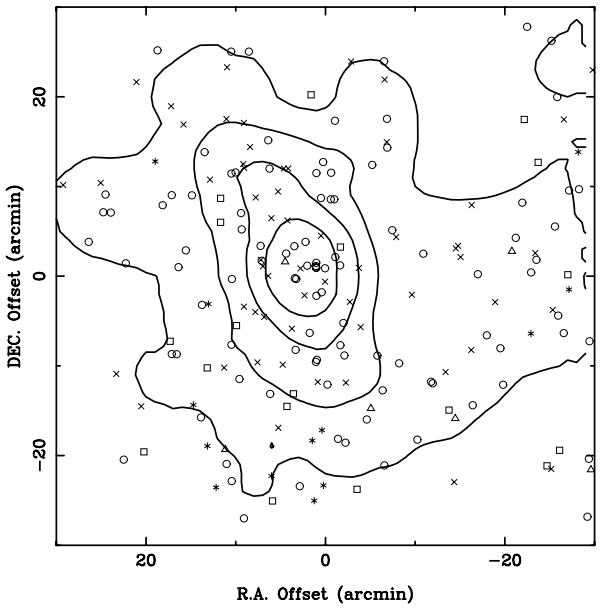

FIG. 10.—Spatial distribution of all member galaxies, including 102 elliptical (*open circles*), 56 lenticular (*crosses*), 13 Sa (*asterisks*), 18 Sb (*open squares*), and six Sc (*open triangles*) galaxies. The contour map of the surface density for all early types using a 5×5 arcmin^2 smoothing window is also given. The contour levels are 0.03, 0.08, 0.13, and 0.18 arcmin^{-2}, respectively.

member galaxies with respect to the central galaxy NGC 7720. Different classes of galaxies are denoted by different symbols. It is easy to see that the early-type galaxies dominate in the central region, exactly superposing on the position of NGC 7720. The contour maps of the surface density for all early-type galaxies, using a 5×5 arcmin^2 smoothing window, are superposed. The contour levels in Figure 10 are 0.03, 0.08, 0.13, and 0.18 arcmin^{-2}, respectively. However, the spatial property of late-type galaxies is significantly dif-

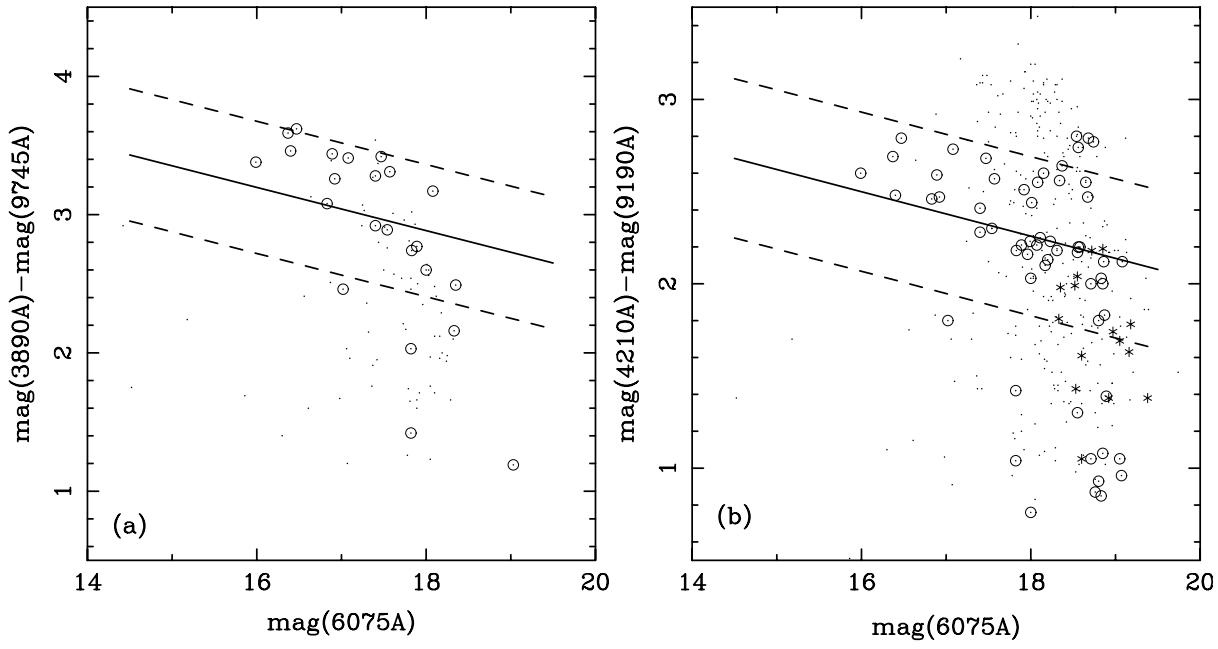

FIG. 9.—Color-magnitude diagram for 359 faint galaxies; 68 early-type member candidates are denoted by open circles, eight spiral galaxies are denoted by asterisks, and the remaining ones are denoted by minor dots. The linear fits with standard errors in color indices in Fig. 4 are also shown.

TABLE 3

SED Catalog of 66 New Member Galaxies in the Central Region of Abell 2634

No.	R.A. (J2000)	Decl. (J2000)	z_{phot}	T	b	c	d	e	f	g	h	i	j	k	m	n	o	p
1	23 36 21.89	27 27 20.65	0.058	1	0.00	20.53	20.00	19.51	19.38	18.93	18.54	18.45	18.39	18.08	17.80	17.93	17.73	17.44
2	23 36 27.48	26 53 41.10	0.003	1	0.00	20.05	19.62	19.37	19.27	18.81	18.80	18.75	18.58	18.43	18.45	18.45	18.25	0.00
3	23 36 27.84	26 40 34.50	0.045	1	19.91	19.27	19.01	18.54	18.34	17.96	17.83	17.75	17.57	17.37	17.28	17.24	17.09	17.17
4	23 36 28.42	26 34 07.31	0.003	1	0.00	20.60	20.02	19.75	19.71	19.21	19.08	18.97	18.84	18.56	18.82	18.87	18.48	0.00
5	23 36 32.23	27 10 37.54	0.058	1	19.98	19.36	18.81	18.26	18.10	17.66	17.47	17.38	17.21	17.00	16.81	16.83	16.68	16.56
6	23 36 32.55	27 14 47.14	0.016	3	20.02	19.55	19.44	19.08	19.00	18.55	18.35	18.23	18.19	18.01	17.92	17.84	17.57	17.53
7	23 36 36.66	26 59 26.97	0.025	3	0.00	20.20	20.10	19.85	19.59	19.40	19.38	19.14	19.02	18.64	19.06	18.61	18.82	0.00
8	23 36 36.66	27 10 29.07	0.016	1	0.00	20.10	19.74	19.30	19.32	18.72	18.56	18.45	18.37	18.11	17.95	18.10	17.90	17.74
9	23 36 37.19	27 01 05.97	0.004	4	19.66	19.29	19.20	18.98	18.86	18.67	18.53	18.51	17.95	18.21	18.15	18.15	17.86	0.00
10...	23 36 41.54	26 56 32.11	0.011	1	0.00	20.16	19.75	19.43	19.25	19.03	18.85	18.68	18.53	18.33	18.39	18.29	18.16	0.00
11...	23 36 41.87	27 20 54.31	0.034	1	0.00	19.70	19.37	18.95	18.78	18.46	18.23	18.09	18.05	17.76	17.71	17.57	17.47	17.45
12...	23 36 42.93	27 06 28.32	0.044	1	0.00	20.48	19.99	19.52	19.23	18.88	18.68	18.48	18.38	18.03	18.07	17.80	17.69	17.51
13...	23 36 43.90	26 57 11.23	0.008	2	0.00	19.78	19.48	19.15	18.97	18.69	18.52	18.43	18.25	18.05	18.04	18.02	17.79	0.00
14...	23 36 44.51	27 27 11.33	0.023	1	0.00	20.00	19.60	19.21	19.00	18.70	18.34	18.18	18.19	17.73	17.73	17.60	17.44	17.47
15...	23 36 44.58	26 39 26.73	0.002	2	0.00	20.05	19.71	19.46	19.21	18.99	18.97	18.86	18.75	18.50	18.58	18.65	18.31	0.00
16...	23 36 50.42	27 13 37.68	0.020	4	19.75	19.34	19.29	19.06	19.00	18.80	18.60	18.52	18.47	18.35	18.28	18.29	18.29	0.00
17...	23 36 51.22	27 02 45.68	0.001	1	0.00	19.60	18.95	18.68	18.59	18.11	17.92	17.81	17.62	17.38	17.35	17.33	17.09	17.07
18...	23 36 51.68	27 03 31.09	0.015	2	0.00	20.13	19.80	19.41	19.22	19.00	18.72	18.66	18.47	18.19	18.23	18.16	17.95	17.85
19...	23 36 53.58	27 01 21.10	0.010	1	0.00	20.46	19.82	19.64	19.36	18.87	18.56	18.49	18.21	18.04	18.09	18.03	17.72	17.65
20...	23 36 53.64	26 54 32.30	0.004	3	10.37	12.02	11.46	11.00	10.33	10.70	10.16	11.01	9.48	9.95	10.45	9.94	8.45	9.01
21...	23 36 55.33	27 28 44.22	0.024	1	0.00	20.06	19.55	19.19	18.93	18.63	18.37	18.18	18.14	17.78	17.67	17.59	17.42	17.22
22...	23 36 57.46	27 09 08.43	0.014	1	19.10	18.15	17.51	17.17	17.10	16.65	16.40	16.30	16.17	15.90	15.81	15.82	15.67	15.64
23...	23 37 00.38	27 05 11.95	0.028	1	0.00	19.50	19.17	18.74	18.55	18.30	18.07	17.99	17.82	17.65	17.50	17.48	17.29	17.29
24...	23 37 06.10	26 48 49.80	0.003	1	19.06	18.64	18.50	18.27	18.04	17.88	17.82	17.66	17.18	17.43	17.30	17.39	17.22	17.03
25...	23 37 07.27	26 52 53.91	0.014	1	0.00	19.97	19.69	19.36	19.06	18.89	18.71	18.53	18.34	18.12	18.21	18.05	17.97	0.00
26...	23 37 37.47	26 49 00.04	0.005	1	0.00	20.00	19.67	19.50	19.19	19.05	18.87	18.82	18.71	18.50	18.51	18.40	18.17	0.00
27...	23 37 41.66	27 03 26.77	0.007	1	0.00	19.43	18.94	18.67	18.48	18.17	17.99	17.87	17.70	17.55	17.45	17.40	17.20	17.30
28...	23 37 44.31	26 42 43.09	0.016	1	0.00	19.75	19.28	18.91	18.53	18.28	18.15	17.92	17.70	17.48	17.36	17.36	17.15	16.90
29...	23 37 52.41	26 51 13.65	0.005	1	19.51	18.69	17.95	17.73	17.49	16.99	16.89	16.74	16.50	16.31	16.25	16.25	16.10	16.07
30...	23 37 57.64	27 15 15.69	0.025	1	0.00	19.40	19.00	18.70	18.49	18.14	17.96	17.83	17.72	17.53	17.46	17.33	17.24	17.08
31...	23 37 57.86	27 18 28.89	0.029	1	0.00	20.47	19.99	19.62	19.37	19.06	18.74	18.51	18.39	18.08	18.02	17.95	17.70	17.73
32...	23 37 59.02	26 39 51.30	0.002	1	18.58	18.00	17.69	17.48	17.26	17.00	17.02	16.88	16.62	16.37	16.38	16.44	16.20	16.12
33...	23 37 59.11	27 24 54.10	0.017	1	19.42	18.64	18.02	17.71	17.59	17.13	16.92	16.79	16.64	16.40	16.34	16.28	16.17	16.16
34...	23 38 02.13	26 52 04.42	0.005	1	19.67	18.77	18.26	18.03	17.80	17.46	17.40	17.25	17.02	16.71	16.71	16.71	16.49	16.39
35...	23 38 04.39	27 13 21.14	0.011	1	19.67	19.05	18.45	18.18	18.03	17.61	17.40	17.31	17.11	16.87	16.76	16.74	16.64	16.75
36...	23 38 11.17	26 37 10.68	0.007	4	18.73	18.37	18.29	18.16	17.96	17.79	17.82	17.56	17.48	17.44	17.41	17.42	17.33	17.31
37...	23 38 18.58	27 04 11.24	0.029	4	19.81	19.44	19.28	19.14	18.97	18.87	18.80	18.83	18.61	18.55	18.60	18.50	18.51	0.00
38...	23 38 19.67	26 42 48.95	0.022	1	20.02	19.28	18.95	18.56	18.38	18.00	18.00	17.83	17.60	17.46	17.45	17.37	17.25	17.42
39...	23 38 21.32	27 09 30.46	0.034	1	19.63	19.01	18.57	18.22	18.02	17.69	17.54	17.36	17.20	17.06	16.93	16.86	16.71	16.74

TABLE 3—*Continued*

No.	R.A. (J2000)	Decl. (J2000)	z_{phot}	T	b	c	d	e	f	g	h	i	j	k	m	n	o	p
40…	23 38 24.37	26 48 51.48	0.022	1	0.00	19.98	19.59	19.17	19.01	18.68	18.55	18.44	18.26	18.10	18.09	17.95	17.81	0.00
41…	23 38 25.44	27 00 19.79	0.015	2	0.00	20.17	19.80	19.46	19.30	18.97	18.85	18.61	18.50	18.25	18.26	18.10	17.98	0.00
42…	23 38 26.15	26 37 36.59	0.005	3	0.00	20.11	19.87	19.74	19.40	19.10	19.16	19.07	18.78	18.75	18.65	18.67	18.48	0.00
43…	23 38 26.29	27 13 39.79	0.022	1	0.00	19.65	19.28	18.84	18.71	18.34	18.11	18.08	17.89	17.65	17.51	17.49	17.40	17.18
44…	23 38 26.80	26 43 46.00	0.012	3	0.00	20.00	19.85	19.57	19.39	19.16	19.05	18.96	18.78	18.48	18.66	18.49	18.31	0.00
45…	23 38 27.19	27 09 39.10	0.043	1	19.97	19.33	18.92	18.56	18.34	18.06	17.89	17.75	17.58	17.41	17.34	17.21	17.12	17.20
46…	23 38 29.09	26 51 36.91	0.007	1	0.00	20.23	19.73	19.51	19.37	18.94	18.83	18.70	18.52	18.41	18.48	18.40	18.20	0.00
47…	23 38 29.48	26 51 23.02	0.014	1	0.00	20.46	19.75	19.51	19.38	18.75	18.65	18.47	18.32	18.10	18.21	18.01	17.91	0.00
48…	23 38 31.11	26 42 36.63	0.004	3	0.00	19.62	19.54	19.35	19.09	19.02	19.07	18.90	18.80	18.59	18.74	18.95	18.66	0.00
49…	23 38 34.15	27 04 45.65	0.032	1	18.60	17.83	17.21	16.80	16.54	16.18	15.99	15.82	15.63	15.47	15.41	15.36	15.23	15.22
50…	23 38 36.74	26 37 31.77	0.005	1	0.00	20.36	19.75	19.50	19.32	18.72	18.67	18.57	18.37	18.20	18.24	18.18	17.89	0.00
51…	23 38 38.53	26 52 43.48	0.018	1	0.00	19.98	19.61	19.24	18.96	18.71	18.58	18.44	18.28	18.09	18.18	17.97	17.78	0.00
52…	23 38 39.57	26 47 49.39	0.009	4	19.64	19.20	19.15	19.05	18.80	18.78	18.76	18.61	18.52	18.50	18.37	18.54	18.33	0.00
53…	23 38 40.25	26 55 05.20	0.014	2	0.00	19.82	19.45	19.10	19.00	18.67	18.55	18.40	18.23	18.06	18.05	17.95	17.78	0.00
54…	23 38 46.24	26 44 02.34	0.014	2	0.00	20.25	20.12	19.76	19.57	19.27	19.18	19.01	18.82	18.73	18.64	18.69	18.47	0.00
55…	23 38 49.31	26 38 40.26	0.005	3	19.65	19.31	19.27	19.12	18.95	18.77	18.83	18.76	18.60	18.49	18.71	18.72	18.46	0.00
56…	23 38 54.17	27 04 18.49	0.038	1	19.07	18.43	17.92	17.52	17.35	17.03	16.83	16.67	16.49	16.30	16.21	16.11	15.97	15.99
57…	23 38 59.41	27 25 57.83	0.042	1	0.00	19.63	19.25	18.73	18.51	18.35	18.01	17.97	17.81	17.47	17.38	17.33	17.19	17.21
58…	23 39 02.95	27 07 58.56	0.012	1	19.11	18.17	17.47	17.22	17.03	16.85	16.37	16.22	15.97	15.74	15.65	15.70	15.48	15.52
59…	23 39 03.60	26 49 28.16	0.008	1	0.00	20.25	19.81	19.45	19.38	18.93	18.86	18.64	18.53	18.36	18.28	18.34	18.13	0.00
60…	23 39 04.95	26 55 25.97	0.029	4	20.06	19.73	19.63	19.41	19.34	19.19	19.05	19.07	19.08	18.87	19.08	18.88	18.68	0.00
61…	23 39 05.28	27 12 29.87	0.048	1	19.16	18.39	17.77	17.39	17.18	16.76	16.47	16.27	16.10	15.87	15.77	15.69	15.60	15.54
62…	23 39 07.27	27 25 57.89	0.003	1	19.65	19.41	19.22	19.00	18.82	18.78	18.55	18.53	18.39	18.30	18.49	18.38	18.11	0.00
63…	23 39 09.27	26 40 00.50	0.011	1	0.00	19.75	19.62	19.43	19.04	18.97	18.89	18.74	18.56	18.45	18.65	18.45	18.36	0.00
64…	23 39 16.71	27 11 42.05	0.032	2	19.92	19.43	19.19	18.87	18.74	18.53	18.33	18.19	18.11	17.86	17.89	17.82	17.62	17.76
65…	23 39 17.87	26 41 59.66	0.005	3	18.74	18.52	18.40	18.28	18.06	17.98	18.00	17.98	17.78	17.72	17.89	17.89	17.76	0.00
66…	23 39 20.31	26 57 43.68	0.034	1	0.00	19.50	19.15	18.83	18.62	18.32	18.17	18.00	17.86	17.68	17.61	17.49	17.40	17.39
67…	23 39 24.18	26 46 35.10	0.003	3	19.65	19.41	19.16	19.09	18.80	18.71	18.71	18.68	18.54	18.39	18.58	18.53	18.36	0.00
68…	23 39 24.76	27 09 57.71	0.040	1	19.99	19.26	18.83	18.38	18.16	17.85	17.57	17.41	17.26	17.04	16.93	16.79	16.69	16.68
69…	23 39 31.55	26 52 14.26	0.012	1	0.00	19.74	19.27	18.96	18.76	18.43	18.31	18.14	17.97	17.82	17.74	17.72	17.56	17.44
70…	23 39 40.15	27 26 06.61	0.057	1	19.54	18.95	18.48	17.90	17.70	17.45	17.08	16.94	16.77	16.54	16.39	16.32	16.22	16.13
71…	23 39 41.18	27 13 44.12	0.004	3	19.88	19.57	19.32	19.02	18.84	18.84	18.60	18.43	18.36	18.24	18.30	18.22	17.96	0.00
72…	23 39 47.39	26 46 25.76	0.004	2	0.00	19.70	19.45	19.31	19.02	18.97	18.92	18.84	18.49	18.51	18.65	18.61	18.32	0.00
73…	23 39 54.29	27 02 22.11	0.023	1	0.00	19.64	19.39	18.97	18.77	18.49	18.20	18.16	17.92	17.85	17.86	17.69	17.51	17.46
74…	23 40 10.83	27 04 45.62	0.055	1	20.40	19.78	19.33	18.72	18.58	18.33	18.08	17.94	17.73	17.55	17.47	17.40	17.23	17.23

ferent from that of the early types. The distribution of spiral galaxies is rather scattered and likely to be located in the outer region of Abell 2634 to the southeast of NGC 7720.

The color-magnitude relation of early-type galaxies has commonly been interpreted as a stellar metallicity effect, in the sense that mean stellar metallicities become progressively higher in brighter galaxies (Arimoto & Yoshii 1987). However, this point of view was recently challenged by a stellar age effect, claimed by Worthey, Trager, & Faber (1995), that the observed color-magnitude relation may result from the younger mean stellar ages in fainter galaxies. Furthermore, Dressler (1980b) found a well-defined relationship between local galaxy density and galaxy type, indicating an increasing elliptical and lenticular population and a corresponding decrease in spiral galaxies with increasing density. Our enlarged sample of member galaxies in the central region of Abell 2634 includes 160 early-type galaxies and 36 spiral galaxies, which allows an illustration on relations between color and magnitude and between local density and galaxy type.

Figure 11*a* shows the color-magnitude relation for all members in the central region of Abell 2634; the relation between color and angular separation, related to NGC 7720 for all members, is given in panel (*b*). The color is represented by the C.I., mag(4210 Å) − mag(9190 Å). The faint blue galaxies, covering the bottom right region of panel (*a*) with C.I. < 2.0 and h mag > 16.5, are dominated by the late-type galaxies. Most of blue galaxies are found to be scattered in the outer region of this cluster, with an angular separation of more than 10′. On the other hand, the dense core of Abell 2634, defined by an angular separation less than 10′, is populated by early-type galaxies, which is also well shown in Figure 10. Our results are consistent with the morphology-density relation found by Dressler (1980b).

It should be stressed that there exists a tendency that the dispersion of color indices of the early-type galaxies becomes larger in the outer region (see panel [*b*]). This phenomenon is first reported in this paper; it might reflect some clues about the *environmental* effect on the evolution of galaxies in a cluster. Assuming that the larger color indices are due to the higher mean stellar metallicities in early-type galaxies, the denser environment in the innermost region is likely to enhance the physical processes that lead to a increase of mean stellar metallicities. The scenario of spiral-spiral merger provides a sound interpretation of the scarcity of late-type galaxies in the core region. We also notice that the reliability of this phenomenon depends on the combined sample. As shown in Figure 9, the galaxies fainter than 16.0 mag are dominant in the list of newly selected members, and they are more likely to have lower color indices, which contributes a lot to the dispersion of color indices. Therefore, it is important to verify this result by taking the follow-up spectroscopic observations of these new member candidates.

6. SUMMARY

This paper presents our multicolor optical photometry for the central region (56′ × 56′) of Abell 2634, using the 60/90 cm Schmidt Telescope of the BAO equipped with 14 BATC filters that cover almost the whole optical wavelength domain. As a result, we obtained the SEDs of 5572 objects. With the help of the NED and the compilations in the literature, we selected 124 known member galaxies from our SED lists, for which the detailed analyses on their SED features are performed. The early-type galaxies are dominant in the central region of Abell 2634. The sample of 59 known early-types offers an opportunity to check the accuracy and reliability of our SED data by the comparison between the observed SEDs and template SEDs. We applied the SED-fitting technique on the 124 known member galaxies to estimate the photometric redshifts and obtained good results: 80% of the members have $z_{\rm phot}$ less than 0.06, which provides a reliable tool for further membership selection. Furthermore, a verification of color-

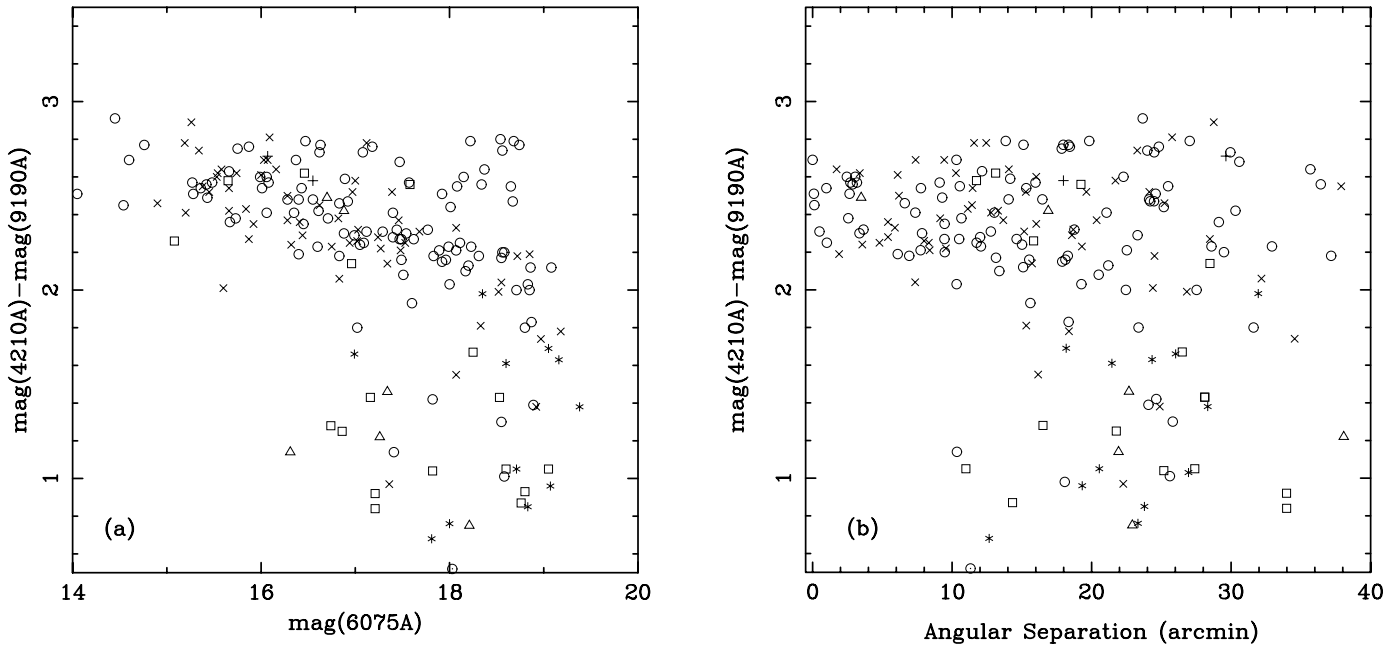

FIG. 11.—(*a*) Color-magnitude relation for all member galaxies. (*b*) The plot of color vs. angular separation (in arcminutes) for all member galaxies. There are 198 member galaxies in our sample, including 102 elliptical (*open circles*), 56 lenticular (*crosses*), two S0a (*plus signs*), 13 Sa (*asterisks*), 18 Sb (*open squares*), six Sc (*open triangles*), and one Irr (*circled dots*) galaxy.

magnitude correlation using our SED information of early-types demonstrates the great advantages and potential for BATC multicolor observations in studying the color-magnitude effect.

Based on the knowledge of SED features of known member galaxies, we carefully used the color-color diagrams, technique of photometric redshift, and color-magnitude correlation (particularly for early-type members) in the selection of faint members. As a result, we isolated 74 galaxies as the faint members, including 58 early types and 16 spiral galaxies. Then, based on the enlarged sample of member galaxies, the spatial distributions for morphologically various galaxies are discussed. We found that most of the blue galaxies are scattered in the outer region of this cluster, and the core region is populated by early-type galaxies for Abell 2634. Furthermore, the color dispersion for early-type galaxies is larger in the outer region, which might be a kind of environmental effect on the evolution of cluster galaxies.

Based on our SED catalogs of known and new members, some studies on the evolution of galaxy populations in the Abell 2634 can be carried out. In order to investigate the dynamics and kinematics of the galaxies in the central region, the follow-up efforts of spectroscopic observations for the sake of obtaining the accurate radial velocities for all the faint member galaxies can be proposed.

This research has made use of the NED, which is operated by the Jet Propulsion Laboratory, California Institute of Technology, under contract with the National Aeronautics and Space Administration. This work is mainly supported by the National Key Base Sciences Research Foundation under contract G1999075402 and is also partly supported by the Chinese National Science Foundation (NSF) under contracts 19873007 and 19873018 to Q. Y. and 19833020 and 19503003 to X. Z. We would like to thank Mr. Yaohua Li, for his management and support of the instruments, and Ray Chen, Haotong Zhang, Bing Zhao, and Zheng Zheng, for obtaining the observational data and sharing their experience with us. We also appreciate the assistants who contributed their hard work to the observations. Furthermore, Q. Y., would like to express his sincere gratitude to Richard Green for the hospitality during his visit to National Optical Astronomy Observatories where the first version of this article was finished, and to Helmut Abt for the help in improving the English writing of this paper.

REFERENCES

Abell, G. O. 1958, ApJS, 3, 211
Arimoto, N., & Yoshii, Y. 1987, A&A, 173, 23
Arnouts, S., Cristiani, S., Moscardini, L., Matarrese, S., Lucchin, F., Fontana, A., & Giallongo, E. 1999, MNRAS, 310, 540
Bertin, E., & Arnouts, S. 1996, A&AS, 117, 393
Bolzonella, M., Miralles, J.-M., & Pelló, R. 2000, A&A, 363, 476
Bower, R. G., Lucey, J. R., & Ellis, R. S. 1992, MNRAS, 254, 589
Butcher, H. R., & Oemler, A. 1978, ApJ, 219, 18
Calzetti, D., Armus, L., Bohlin, R. C., Kinney, A. L., Koornneef, J., & Storchi-Bergmann, T. 2000, ApJ, 533, 682
Dressler, A. 1980a, ApJS, 42, 565
———. 1980b, ApJ, 236, 351
Dressler, A., Lynden-Bell, D., Burstein, D., Davies, R. L., Faber, S. M., Terlevich, R. J., & Wegner, G. 1987, ApJ, 313, 42
Eilek, J. A., Burns, J. O., O'Dea, C. P., & Owen, F. N. 1984, ApJ, 278, 37
Fan, X., et al. 1996, AJ, 112, 628
Fukugita, M., Ichikawa, T., Gunn, J. E., Doi, M., Shimasaku, K., & Schneider, D. P. 1996, AJ, 111, 1748
Furusawa, H., Shimasaku, K., Doi, M., & Okamura, S. 2000, ApJ, 534, 624
Griffen, R. F. 1963, AJ, 68, 421
Gunn, J. E., & Stryker, L. L. 1983, ApJS, 52, 121
Huang, H., et al. 2001, in preparation
Kinney, A. L., Calzetti, D., Bohlin, R. C., McQuade, K., Storchi-Bergmann, T., & Schmitt, H. R. 1996, ApJ, 467, 38
Lanzetta, K. M., Yahil, A., & Fernández-Soto, A. 1996, Nature, 381, 759
Lucey, J. R., Gray, P. M., Carter, D., & Terlevich, R. J. 1991, MNRAS, 248, 804
Lucey, J. R., Guzmán, R., Steel, J., & Carter, D. 1997, MNRAS, 287, 899
Matthews, T. A., Morgan, W. W., & Schmidt, M. 1964, ApJ, 140, 35
O'Donoghue, A., Owen, F. N., & Eilek, J. 1990, ApJS, 72, 75
Oke, J. B., & Gunn, J. E. 1983, ApJ, 266, 713
Paturel, G., et al. 1997, A&AS, 124, 109
Pinkney, J., Rhee, G., Burns, J. O., Hill, J. M., Oegerle, W., Batuski, D., & Hintzen, P. 1993, ApJ, 416, 36
Scodeggio, M., Giovanelli, R., & Haynes, M. 1997, AJ, 113, 101
———. 1998, AJ, 116, 2738
Scodeggio, M., Solanes, J. M., Giovanelli, R., & Haynes, M. P. 1995, ApJ, 444, 41 (SSGH)
Struble, M. F., & Rood, H. J. 1999, ApJS, 125, 35
Wegner, G., Haynes, M. P., & Giovanelli, R. 1993, AJ, 105, 1251
Worthey, G. Trager, S. C., & Faber, S. M. 1995, in ASP Conf. Ser. 86, Fresh Views of Elliptical Galaxies, ed. A. Buzzoni, A. Renzini, & A. Serrano (San Francisco: ASP), 203
Yan, H., et al. 2000, PASP, 112, 691
Zhou, X., Chen, J. S., Xu, W., Zhang, M., Jiang, Z. J., & Zhu, J. 1999, PASP, 111, 909
Zhou, X., et al. 2001, PASJ, submitted